Journal of Energy Storage 72 (2023) 108614

Contents lists available at ScienceDirect

Journal of Energy Storage

journal homepage: www.elsevier.com/locate/est

Research papers

Cost-optimal Power-to-Methanol: Flexible operation or intermediate storage?

Simone Mucci [a], Alexander Mitsos [b,a,c], Dominik Bongartz [d,*]

[a] Process Systems Engineering (AVT.SVT), RWTH Aachen University, 52074 Aachen, Germany
[b] JARA-ENERGY, 52056 Aachen, Germany
[c] Energy Systems Engineering (IEK-10), Forschungszentrum Jülich, 52425 Jülich, Germany
[d] Department of Chemical Engineering, KU Leuven, 3001 Leuven, Belgium

ARTICLE INFO

Keywords:
Power-to-Methanol
Flexibility
Hydrogen storage
Battery
Combined design and scheduling optimization
Specific cost of methanol

ABSTRACT

The synthesis of methanol from captured carbon dioxide and green hydrogen could be a promising replacement for the current fossil-based production. The major energy input and cost driver for such a process is the electricity for hydrogen production. Time-variable electricity cost or availability thus motivates flexible operation. However, it is unclear if each unit of the process should be operated flexibly, and if storage of electricity or hydrogen reduces the methanol production cost. To answer these questions, we modeled a Power-to-Methanol plant with batteries and hydrogen storage. Using this model, we solved a combined design and scheduling optimization problem, which provides the optimal size of the units of the plant and their optimal (quasi-stationary) operation. The annualized cost of methanol was minimized for a grid-connected and a stand-alone case study considering current and future (2030) unit cost scenarios. The optimization results confirm that storage, especially hydrogen storage, is particularly beneficial when the electricity price is high and highly fluctuating. In future unit cost scenarios, batteries could play an even bigger role due to the expected significant cost reduction. Irrespective of the presence of storage, the whole Power-to-Methanol plant should be operated flexibly: even moderate flexibility of the methanol synthesis unit significantly reduces the production cost.

1. Introduction

Methanol is a promising liquid energy carrier [1] due to its relatively high volumetric and gravimetric energy density and simple handling, but it has a significantly lower roundtrip efficiency when compared with other energy storage technologies, e.g., batteries [2]. Nevertheless, even when it is not converted back to electricity, methanol plays a big role as a platform chemical since it is widely used for the synthesis of several products, e.g., formaldehyde, dimethyl ether, and plastics and has high potential as alternative fuel or for the production of other liquid fuels, e.g., gasoline and jet fuel [3].

Nowadays, methanol production mostly relies on fossil feedstocks, e.g., natural gas and coal [3], therefore, the defossilization of its chemical production process is essential. Methanol from biomass (bio-methanol) and electricity-based methanol (e-methanol) could help achieve this environmental goal for the chemical industry. Bio-methanol production is, however, limited by the availability of residual biomass, which could also be used to produce more complex molecules and products [4,5]. E-methanol production relies on a CO_2 source and renewable electricity availability: CO_2 can be obtained from point sources or from air [6], while renewable electricity can be supplied by stand-alone and grid-connected generation parks. Because of the expected increase of installed renewables [7] and the abundance of CO_2 sources, e-methanol production (Power-to-Methanol) is considered in this work.

Power-to-Methanol plants require high electricity input to produce hydrogen via electrolysis. Because of this high electricity demand and the high flexibility of methanol plants [8–10], demand-side management [11,12] could be applied to reduce the production cost or to synthesize the product according to the power availability [13]. However, time-variable operation requires oversizing the plant for a fixed overall production rate. Thus, the extent to which the plant is operated flexibly has to be chosen carefully to balance operating and capital costs [10]. Oversizing of the electricity-demanding units combined with a product or intermediate storage has often been proposed to deal with renewables or fluctuating prices in different applications, e.g., chlor-alkali electrolysis [14], Power-to-Fuel plants [15,16], and ammonia production processes [17,18]. Storage technologies, e.g., batteries and tanks

* Corresponding author.
E-mail address: dominikbongartz@alum.mit.edu (D. Bongartz).

https://doi.org/10.1016/j.est.2023.108614
Received 22 May 2023; Received in revised form 1 August 2023; Accepted 3 August 2023
Available online 18 August 2023

Table 1
Relevant combined design and scheduling optimization works for the main Power-to-X processes with storage.

	Power-to-X process	Grid-connected	Stand-alone	Battery	Hydrogen storage	Other storage technologies	X-process flexibility	Scheduling horizon	Problem formulation
Li et al. [22]	P-to-NH_3	No	Yes	No	Yes	No	Yes	1 day	LP
Schulte Beerbühl et al. [23]	P-to-NH_3	Yes	No	No	Yes	No	Yes	1 year	NLP
Osman et al. [24]	P-to-NH_3	No	Yes	Yes	Yes	Yes	No	1 year	LP
Allman et al. [17][25]	P-to-NH_3	No	Yes	No	Yes	Yes	Yes	2-day moving horizon for 1 year	MILP
Chen et al. [26]	P-to-CH_3OH	Yes[a]	Yes	No	Yes	No	No	1 year	NLP
Chen and Yang [27]	P-to-CH_3OH	Yes[a]	Yes	No	Yes	Yes	Yes	1 year	LP
Svitnič and Sundmacher [28]	P-to-CH_3OH	No	Yes	Yes	Yes	Yes	Yes	Time series aggregation	LP
This work	P-to-CH_3OH	Yes	Yes	Yes	Yes	No	Yes	60 days	MINLP

[a] Renewable plant as the main energy source; electricity grid as energy backup, but no hourly price variability was considered.

for intermediates, in support of Power-to-Methanol plants could therefore contribute to reducing the production cost of methanol. In fact, batteries can decouple electricity production from its utilization, while intermediate hydrogen storage can decouple hydrogen production from its conversion into methanol.

While batteries and hydrogen storage systems are frequently used and optimized in microgrids [19] and multi-energy systems [20] to cope with renewables and variable loads, few works about hydrogen storage and plant capacity optimization are found in the Power-to-Chemical field (Table 1), for example, for Power-to-Gas [21] and Power-to-Ammonia [22,23] plants. The interplay between batteries and hydrogen storage has been investigated for Power-to-Ammonia plants: both storage technologies were chosen by the Cplex optimizer for a case study in which the production rate of ammonia was assumed constant [24], while either the hydrogen storage or both storage technologies were chosen according to the solving method and case study in another work [25]. As regards Power-to-Methanol, Chen et al. [26,27] optimized the design of a plant also including hydrogen storage for several scenarios. A more extended Power-to-Methanol process network with multiple components and storage technologies, including hydrogen storage and batteries, was optimized by Svitnič and Sundmacher [28]. However, in these works [26–28], the model of highly nonlinear components of the Power-to-Methanol plant is linearized and the integer variables, which allow setting the operating limits of the units, are avoided. This formulation makes, on the one hand, the optimization problem easier to solve, on the other hand, the results less accurate. Furthermore, these works do not investigate the possibility of optimally exploiting electricity price variations in grid-connected Power-to-Methanol plants with storage to minimize the methanol production cost. Therefore, it is not clear whether batteries and hydrogen storage are always beneficial from an economic perspective, especially in grid-connected plants, and if and to what extent the methanol synthesis unit should be operated flexibly even in their presence.

To tackle these questions and address the literature shortcomings, we modeled a Power-to-Methanol plant with both a battery and hydrogen storage (Fig. 1) in GAMS [29] based on mass and energy balances and performance models for the units. The resulting mixed-integer nonlinear programming (MINLP) problem considers combined design (in particular sizing) and scheduling, accounting for the operating limits of every unit, thus fully exploiting the potential of flexible operation [30]. We then optimized with BARON [31] the design of a grid-connected and stand-alone Power-to-Methanol plant for single scheduling scenarios to investigate how the optimal plant design depends on these. The specific cost of methanol was used as the objective function and as the metric to compare different configurations and case studies.

The remainder of the paper is structured as follows: in Sections 2 and 3, the investigated Power-to-Methanol plant and its model are described; Sections 4 and 5 present the case studies and the formulation of the optimization problems, while in Sections 6 and 7, the optimization results are analyzed and the conclusions are drawn. Furthermore, additional information and the GAMS code are provided in Appendix and Supplementary Information.

2. System description

The investigated Power-to-Methanol concept (Fig. 1) is composed of three key units, i.e., the water electrolyzer, the compression unit, and the methanol synthesis plant. Additionally, a battery and hydrogen storage are considered to investigate their role. A short description of these units is provided in the following subsections.

2.1. Battery

Electricity can be stored electrochemically in batteries in order to be used in following periods. Different battery technologies have been developed for energy storage and automotive purposes [2]. For the current work, we considered a lithium-ion type battery because of the high roundtrip efficiency (around 95%), high technological readiness level due to the production on a large scale, and the expected cost drop [2,32].

2.2. PEM water electrolyzer

The water electrolyzer is the key component of the investigated Power-to-Methanol concept. Among alternative electrolysis technologies, we chose Polymer Electrolyte Membrane water electrolyzers (PEM-WE) since they have high technological maturity and efficiency, wide operating limits [33], and they are reported to be particularly suitable to follow variable power inputs [34,35].

Furthermore, PEM-WEs can be operated at relatively high pressures. On the one hand, pressurized electrolyzers have a lower efficiency (higher operating costs); on the other hand, they reduce the size and cost of the downstream compression unit. The trade-off between higher capital or operating cost depends on the considered boundary conditions, e.g., electricity cost and delivery hydrogen pressure, and will be investigated for the considered Power-to-Methanol plant.

2.3. Hydrogen compression unit

Hydrogen has to be compressed from the pressure at the outlet of the electrolyzer up to the delivery pressure. Although several compression technologies are available, e.g., mechanical and electrochemical compression, only reciprocating and centrifugal hydrogen compressors have reached a high technological maturity on a large scale [36]. We selected centrifugal compressors because of their high reliability and capability of handling high hydrogen flow rates.

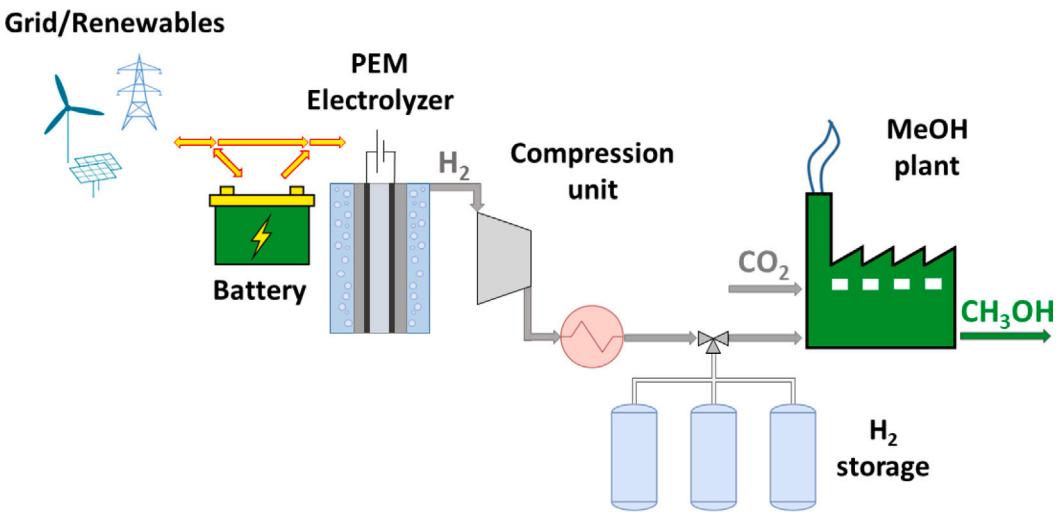

Fig. 1. Sketch of the Power-to-Methanol plant with battery and hydrogen storage. The plant configurations with only the battery, with only the hydrogen storage, and without any storage were also considered (not shown here).

The delivery pressure of hydrogen that the compression unit has to reach varies according to the plant configuration. In absence of hydrogen storage, the delivery pressure matches the operating pressure of the methanol synthesis plant (75 bar). In case intermediate H_2 storage is present, the delivery pressure varies over time according to the pressure inside the storage.

For the considered case studies, a compression unit without intermediate cooling is sufficient to supply hydrogen at the delivery pressure. The compressed hydrogen is then cooled to 25 °C before being injected into the hydrogen storage or supplied to the methanol synthesis plant.

2.4. Hydrogen storage

Hydrogen can be stored either physically, i.e., as liquid or gas, or in some materials via chemical or physical sorption [37]. We chose physical-based storage for the considered application since it is the most mature technology [37].

Storing hydrogen as a liquid allows for increasing its energy density, thus reducing the size of the storage. However, this solution requires a dedicated liquefaction plant, which significantly increases the overall plant complexity and cost. Instead, gaseous storage does not need dedicated plants except for a compression unit. There are two main gaseous storage alternatives, i.e., above-ground in vessels and underground in caverns [37,38]. The use of pressurized vessels was chosen since it is geographically unconstrained. Among the several types of above-ground hydrogen storage [37,39], hydrogen vessels of type I [37] are the most suitable for stationary applications for the pressure range of interest (maximum pressure below 200 bar) as they are the cheapest.

2.5. Methanol synthesis plant

Methanol can be produced from carbon dioxide and hydrogen either directly or indirectly. In the direct route, CO_2 is directly converted to methanol via hydrogenation. In the indirect route, CO_2 is first reduced to carbon monoxide either thermochemically or electrochemically and then mixed with hydrogen to produce syngas that is converted to methanol. The intermediate production of syngas aims at using the consolidated know-how of methanol production from fossil fuels, e.g., natural gas. The direct pathway is gaining relevance in the last decades because of the lower plant complexity, overall efficiency, and economic feasibility [40]. For this reason, the direct hydrogenation of CO_2 to methanol pathway was chosen.

3. Model

The Power-to-Methanol plant with storage is modeled via mass and energy balances and by considering discrete time dynamics. We assumed quasi-stationary operation for each unit except for storage. Also, cost functions are used to estimate capital and operating costs. The overall model was not linearized to obtain more accurate results since some equations are highly nonlinear. In this section, the main modeling equations of each unit are presented. For the complete model and the GAMS code, we refer to the Supplementary Information.

3.1. Battery

The battery is modeled via the energy balance

$$E_b(t) = E_b(t-\Delta t)\cdot(1-r_{self-disch}) + P_{in}(t)\cdot\eta_{ch}\cdot\Delta t - \frac{P_{out}(t)}{\eta_{disch}}\cdot\Delta t,$$

where $E_b(t)$ is the energy content, $P_{in}(t)$ the power input from the grid, $P_{out}(t)$ the power in DC that can be effectively used, and Δt the discretization time step. The values for the charging (η_{ch}) and discharging (η_{disch}) efficiencies and the self-discharge rate ($r_{self-disch}$) were considered constant (see Supplementary Information). The hourly self-discharge rate was estimated by considering an energy loss of 0.2% per day [2]. Other modeling approaches, e.g., efficiencies as a function of the current and of the state of charge of the battery [41], would have improved the accuracy but also increased the complexity of the optimization problem.

The power output of the battery can be supplied to the water electrolyzer ($P_{to-PEM}(t)$) or to the grid ($P_{to-grid}(t)$) if converted from DC to AC:

$$P_{out}(t) = \frac{P_{to-grid}(t)}{\eta_{DC-AC}} + P_{to-PEM}(t).$$

The capital cost of the battery was estimated from its nominal capacity. The specific cost of 310 $/kWh (the average installation cost of utility-scale stationary battery systems in 2020 [32]) was considered and updated to the reference year (2021).

3.2. PEM water electrolyzer

The water electrolysis unit is composed of several electrolysis modules. The main specifications of the considered electrolyzer module are summarized in Table 2. The PEM water electrolyzer module was modeled by considering the equations and parameters in Järvinen

Table 2
Main specifications of the considered PEM water electrolyzer module.

	Values
Operating temperature	75 °C
Operating pressure range	20–40 bar
Nominal power per module	2.0 MW
Maximum power per module	2.5 MW

et al. [42]. Two additional assumptions were made: i) the Faradaic efficiency is equal to one, and (ii) the pressure dependency is considered in the Nernst equation only.

Since the equation-based model contains several variables that are unnecessary for the current scope and would slow down the optimizer, we replaced the electrolyzer model with a polynomial fit of its efficiency (based on the lower heating value, see Appendix A.1). The electrolyzer efficiency was then used to calculate the hydrogen mass flow rate, the power, and cooling demand.

Additional operating costs were considered for the auxiliaries, e.g., the power electronics units and pumps. In particular, the additional energy consumption was assumed equal to the 5% of the electricity needed to operate the electrolyzer (constant value for the whole operating range of the electrolyzer).

The capital cost of the PEM electrolyzer was calculated by multiplying the nominal power of the electrolyzer by the specific cost in €/kW, which was calculated with the correlation proposed by Reksten et al. [43]. The maximum power of the electrolyzer could have been used in the correlation for a more conservative cost estimation. In fact, PEM electrolyzers can be operated at a maximum power significantly higher than the nominal one (up to 150% [35]; 125% in our case, see Table 2), even though for a limited amount of time [35]. However, the value of the nominal power of the electrolysis unit is generally considered in these correlations. To also take into account civil works and installation costs, a multiplying factor of 1.75 was assumed. Additionally, a second electrolysis unit is considered to be purchased in the tenth year, since the typical lifetime of PEM electrolyzers (30–90 kh [33]) is shorter than the typical lifetime of the chemical plant (20–30 years). This choice indirectly accounts for accelerated degradation when the electrolyzer is operated flexibly since the electrolysis unit is substituted in the tenth year although the number of yearly equivalent operating hours is lower than when it is constantly operated in steady state (8000 h/y).

3.3. Hydrogen compression unit

A multi-stage centrifugal compressor was considered in the plant. This compression technology has an operating range of around 50%–100% [36] if variable rotating speed [44] or variable inlet guide vanes [45] are used. As the other units have a wider operating range, the operation of two compressors in parallel was considered to extend it to 25%–100%, although this affects the capital cost of the unit (economy of scale). The use of a low-pressure buffer tank before the compression unit was not considered, although it would have further increased the flexibility of the plant.

The overall power of compression ($P_{\mathrm{comp}}(t)$) is calculated as follows:

$$P_{\mathrm{comp}}(t) = \dot{m}_{\mathrm{H_2}}(t) \cdot \frac{c_{\mathrm{p}} \cdot T_{\mathrm{in}}}{\eta_{\mathrm{is}} \cdot \eta_{\mathrm{mec}}} \cdot \left(\beta(t)^{\left(\frac{k-1}{k}\right)} - 1 \right),$$

where $\dot{m}_{\mathrm{H_2}}(t)$, c_{p}, and k are the hydrogen mass flow rate, the specific heat at constant pressure, and the heat capacity ratio of hydrogen, respectively, T_{in} the hydrogen temperature at the inlet of the compression unit (assumed equal to 298 K), $\beta(t)$ the pressure ratio, and η_{is} and η_{mec} the isentropic and mechanical efficiencies. The isentropic efficiency was assumed constant over the operating range and conservatively equal to 0.8 [36,44]. A validation of the model of the compressor can be found in Appendix A.2.

The pressure ratio is determined by the operating pressure of the electrolyzer and the pressure inside the hydrogen storage unless a bypass of the hydrogen storage is considered. With a bypass, some compression energy could be saved depending on the electricity price, the operating load of the methanol synthesis plant, and the pressure inside the storage. However, this configuration was not considered in this work. Also, no hydrogen losses were considered during the compression phase since they are lower than 0.5% [36].

The compressed hydrogen is then cooled in a single heat exchanger to 298 K. The cooling demand was assumed equal to the power needed for compression. The capital cost of these components was estimated at the maximum flow rate condition by using the cost models proposed by Biegler et al. [46].

3.4. Hydrogen storage

The amount of hydrogen available in the vessel ($M_{\mathrm{H_2}}(t)$) is calculated with the following mass balance:

$$M_{\mathrm{H_2}}(t) = M_{\mathrm{H_2}}(t - \Delta t) + \dot{m}_{\mathrm{H_2,prod}}(t) \cdot \Delta t - \dot{m}_{\mathrm{H_{2,MeOH}}}(t) \cdot \Delta t,$$

where $\dot{m}_{\mathrm{H_{2,prod}}}(t)$ is the hydrogen flow rate produced by the electrolyzer, and $\dot{m}_{\mathrm{H_{2,MeOH}}}(t)$ the hydrogen flow rate consumed in the methanol synthesis plant.

The hydrogen storage was assumed isothermal at 298 K, and the pressure inside the storage ($p(t)$) was estimated from the available hydrogen inside the storage by using a linear interpolation of the density (ρ) (Appendix A.2). As the methanol synthesis occurs at a pressure of 75 bar, the minimum pressure of the storage is set to that value. The available hydrogen stored in the vessel at the time step t and its pressure are, therefore, calculated as follows:

$$M_{\mathrm{H_2}}(t) = V \cdot \left(\rho_{(\mathrm{p(t)})} - \rho_{(75\ \mathrm{bar})} \right) \approx V \cdot 0.073\ \frac{\mathrm{kg}}{\mathrm{m^3 bar}} \cdot (p(t) - 75\ \mathrm{bar}),$$

where V is the volume of the storage, which was considered as a continuous variable, even though multiple hydrogen vessels of limited size would be probably needed in large-scale plants [38].

The capital cost of the storage was estimated by using the specific cost per unit of volume. Further details can be found in Appendix A.3.

3.5. Methanol synthesis plant

The methanol synthesis plant was modeled in Aspen Plus® V11 (see Appendix A.4 for more details). However, such a detailed model cannot be embedded in GAMS and handled by the optimizer. Therefore, the key information about efficiency, mass flow rates, and energy demand was extracted to build a simplified algebraic model of the plant. In particular, the produced methanol mass flow rate depends linearly on the hydrogen flow rate (assumption of constant efficiency for the methanol synthesis plant), while the electricity demand, the cooling demand, and the inlet CO_2 mass flow rate scale linearly with the methanol production rate. The efficiency of the methanol synthesis plant is assumed constant in the operating range since it is not expected to have significant changes when varying the methanol plant load, especially if relatively low ramp rates (< 50%/h) are considered [9]. The complete model can be found in the GAMS file provided in the Supplementary Information.

While the H_2 production is simulated by the model of the electrolysis unit (Section 3.2), the model of the carbon capture unit for the CO_2 supply was not included in the optimization problem. Therefore, it was assumed that a suitable CO_2 stream can be supplied to the methanol synthesis plant at every time step.

The capital cost of the methanol synthesis plant (CAPEX) was estimated by using the Aspen Plus model (Appendix A.4) as the reference in the regression function, which is defined as:

$$\mathrm{CAPEX} = \mathrm{CAPEX_{ref}} \cdot \left(\frac{\mathrm{M_{MeOH}}}{\mathrm{M_{MeOH,\ ref}}} \right)^{\mathrm{b}},$$

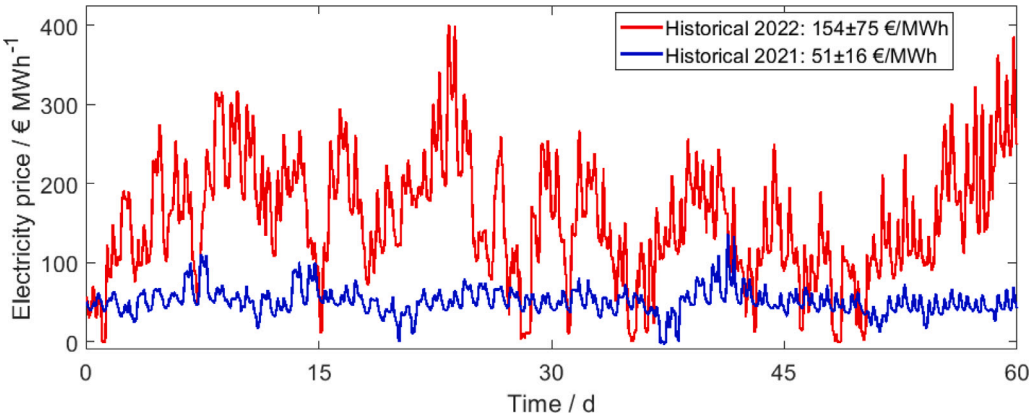

Fig. 2. Electricity price scenarios [49].

where b is the regressive exponent (equal to 0.6 for the six-tenths rule), to evaluate the CAPEX for different plant capacities (M_{MeOH}). Further details about the cost estimation can be found in Appendix A.5.

4. Case studies

The production of e-methanol as a platform chemical was investigated via the Power-to-Methanol model described in Section 3. The role of storage and flexibility in the Power-to-Methanol plant was analyzed for two case studies, i.e., grid-connected and stand-alone plants.

For both case studies, two-month scenarios were considered and discretized with hourly resolution (1440 time steps) for the scheduling problem. The relatively short time frame is motivated by the size of the optimization problems (the number of variables and constraints scale linearly with the number of time steps unless time-aggregation series techniques are used [47]) and by the fact that no seasonal storage of hydrogen and electricity is expected. In fact, as the investment cost for storage scales with its size and methanol is the final product, the methanol plant is most likely operated almost continuously, thus meaning that the stored H_2 and electricity will be used in a relatively short term in case the electricity is expensive or the renewable power is not sufficient to produce enough hydrogen via electrolysis for the methanol plant. Nevertheless, this time frame allows considering price and renewable power variations that occur on different time scales, e.g., electricity price variation between working and weekend days for multiple weeks, and the diurnal effects on renewable power generation. Furthermore, as the plant units have high ramp rates and fast dynamics [2,8,9,35][48] compared with the considered time step (1 h), quasi-stationarity at the operating points was assumed: the plant is considered in steady-state at each time step independently from the operating point at the previous time step.

For the grid-connected case study, we assumed that there are no limitations in terms of power availability, and that the amount of energy exchanged with the grid does not affect the electricity price. Two electricity price scenarios based on historical day-ahead electricity prices of Germany (the first 60 days of the years 2021 and 2022, bidding zone BZN|DE-LU of Germany [49]) were analyzed. The scenarios differ significantly in terms of mean value and standard deviation (Fig. 2), representing a low-price scenario with a small standard deviation, and a high-price scenario with a high standard deviation. Although producing low carbon footprint e-methanol is desirable, high penetration of renewables in the electricity grid is not a necessary assumption for this work since we used methanol production cost as the metric. Nevertheless, the considered electricity price profiles are intended to be two possible and very different indications of future electricity price scenarios when the carbon footprint of the electricity will be lower.

For the stand-alone case study, the power is assumed to be produced by a dedicated renewable generation park composed of wind and photovoltaic plants. The considered power generation profiles (Fig. 3) do not belong to any specific power plant, but they were taken from German historical data (May–June 2022 and November–December 2022, bidding zone BZN|DE-LU of Germany [49]) and scaled to a typical size for large renewable parks (126 MW and 110 MW in nominal conditions for wind and photovoltaic plants, respectively). The considered profiles were chosen to represent the two extremes, i.e., renewable generation in summer (characterized by high peaks due to photovoltaic plants) and in winter (when wind power production plays the major role), since no yearly seasonality could be considered in a single scheduling scenario due to computational issues. Furthermore, the complementarity of photovoltaic and wind power generation throughout the year also reduces the production costs [28] and the need for seasonal (hydrogen) storage, thus meaning the estimated size of storage in the two-month scenario might be most likely sufficient. Additional assumptions were made: i) the forecast of the energy production from the renewable generation park is perfect, ii) the cost of electricity is null since the capital cost of the renewable plants [50] and the O&M expenditures are included in the methanol production cost calculation, iii) the sum of the electricity demand of the whole Power-to-Methanol plant must be less than or equal to the electricity available for each time step; iv) electricity in the battery can also be converted to AC to supply energy to the methanol synthesis plant in case of renewable production shortage; v) the eventual excess of electricity is curtailed.

To investigate the role of storage, four plant configurations were considered, i.e., the Power-to-Methanol plant without storage, with a battery, with H_2 storage, and with both storage technologies (Fig. 4) in the grid-connected case study. In the stand-alone case study instead, only the Power-to-Methanol plant configuration with both storage technologies was considered since storage is essential to grant continuous operation of the downstream plant. In fact, the battery can supply energy to the plant in case of a temporary electricity generation shortage, while the H_2 vessel can supply H_2 to the methanol synthesis plant when the electricity production is not sufficient to run the electrolysis unit.

Furthermore, as the investment cost of some of the units is expected to have a significant reduction due to the high learning rates, the optimization problems were also solved by considering capital cost predictions for the year 2030 (Scenario 2030). The assumed values can be found in Appendix A.6.

Finally, the annualized cost of methanol (C_{MeOH}) was used as a metric to compare the configurations for each case study. It is defined as:

$$C_{MeOH} = \frac{CAPEX_0 + CAPEX_{PEM} \cdot (1+i)^{-10} + \sum_{j=1}^{N} (O\&M + OPEX_y) \cdot (1+i)^{-j}}{\sum_{j=1}^{N} (M_{MeOH,\,y}) \cdot (1+i)^{-j}},$$

where $CAPEX_0$, O&M, and $OPEX_y$ are the initial capital expenditures, the yearly operation and maintenance, and the operating costs of the

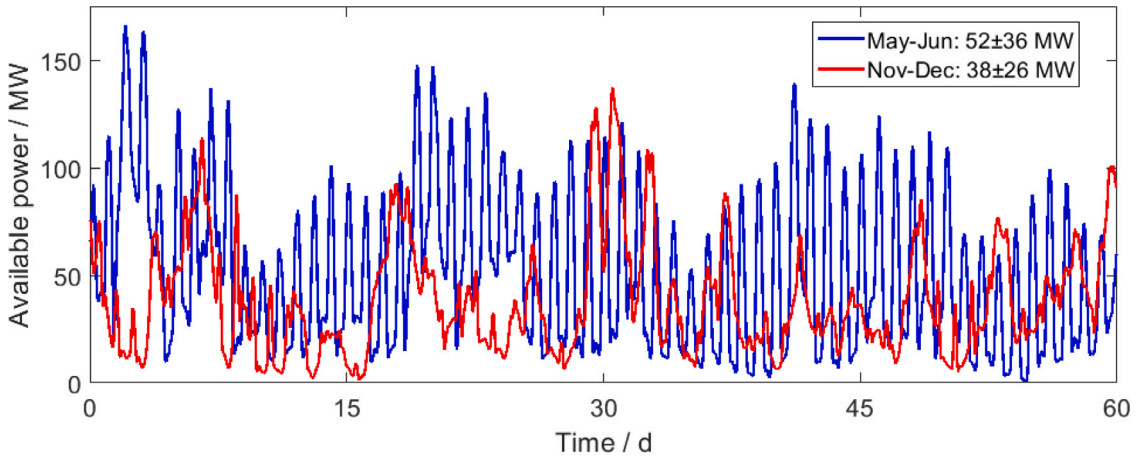

Fig. 3. Power availability scenarios [49].

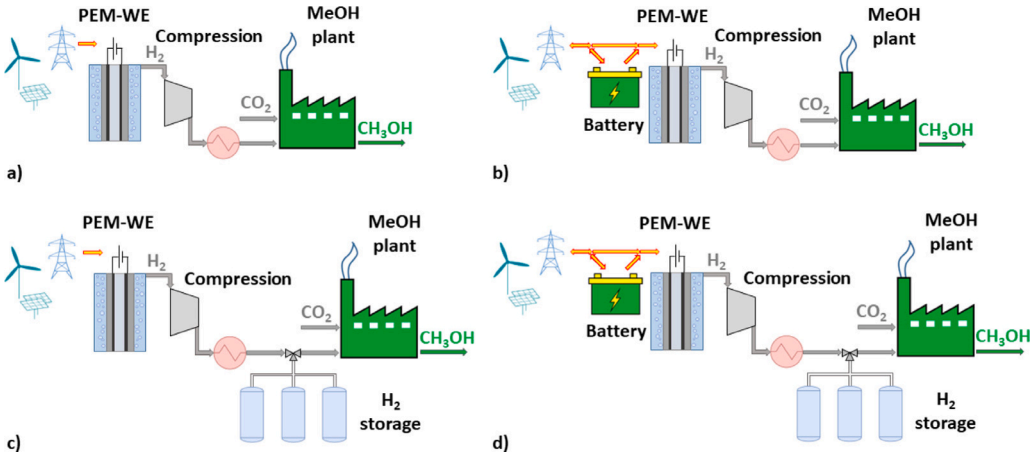

Fig. 4. Investigated Power-to-Methanol plant configurations: a) without any storage, b) with a battery, c) with H_2 storage, and d) with battery and H_2 storage.

plant, respectively, N the number of operating years, $M_{\mathrm{MeOH,\,y}}$ the yearly production of methanol, and i the discount rate. Additionally, a replacement of the electrolysis unit at the end of the tenth year is considered (see Section 3.2). No salvage value of the plant was considered in order to have a conservative estimation of the methanol production cost. The capital cost of the single units was calculated with the cost models described in Section 3 as the result of the optimal design. The operating costs were calculated as the result of the optimal scheduling as well as the methanol production. In fact, no methanol production target was set in order not to limit the economic savings from scheduling. Therefore, methanol production is mainly limited by the ranges of the optimization variables, e.g., the size of the electrolysis unit, or the availability of renewable energy. Nevertheless, a minimum value of 40 kt/y, half of the maximum methanol production for the considered boundaries, was set for the grid-connected case studies to avoid not meaningful solutions with the assumed cheap future cost of batteries (see Section 6). Further assumptions for the economic evaluations are summarized in Table 3.

Table 3
Main assumptions for the economic evaluations.

	Values
Operating weeks per year for the methanol synthesis plant	48 w/y
Lifetime of the Power-to-Methanol plant	20 y
Yearly O&M as % of the initial $CAPEX_0$	5%
Discount rate i	5%
\$ to € conversion factor	0.85
Cooling cost	1 €/MWh
CO_2 stream cost	50 €/t [3]

5. Optimization

The combined design and scheduling optimization problems were formulated in GAMS 38.2.1 [29] and solved on an Intel Xeon Gold 6226 CPU with 2.7 GHz and 384 GB RAM. These MINLP problems were initialized with a starting solution found after a multi-start local search and then solved with the global optimizer BARON, version 22.2.3 [31]. Two stopping criteria were considered for the optimizer, i.e., an optimality gap of 0.01 and the CPU time limit of 12 h. Unfortunately, the relative difference between the upper bound (best feasible solution found) and the lower bound (best possible solution) did not reach the required optimality gap within the computational time limit in most of the optimization problems, thus, overall global optimality cannot be guaranteed. Nevertheless, the upper bound stabilized after a few iterations, thus suggesting that the convergence issues were mainly due to the difficulty of proving global optimality with wide variable bounds (global optima were proven in some of the problems after tightening the variable bounds). In preliminary analyses, we also tested Knitro,

Table 4
Design and scheduling variables of the optimization problem for the grid-connected and stand-alone case studies. A short description of the variable and the considered upper and lower bounds are also provided.

Unit	Symbol	Description of the design variable	Min value	Max value
Battery	$E_{b,nom}$	Energy capacity	5 MWh	400 MWh
PEM-WE	N_{mod}	Number of modules	10	40
	p_{PEM}	Operating pressure	20 bar	40 bar
H_2 compression	β_{max}	Maximum pressure ratio	1.88	3.50
H_2 storage	V	Volume of the vessel	25 m^3	7500 m^3
	$\dot{m}_{H_{2,MeOH},nom}$	Nominal H_2 flow rate for the methanol synthesis plant	0.4 t/h	2 t/h

Unit	Symbol	Description of the scheduling variable	Min value	Max value
Battery	$P_{in}(t)$	Power input	0.5 MW[a]	min(100 MW, $(0.9 \cdot E_{b,nom}/1h)$)
	$x_{b,in}(t)$	Binary to decide when the battery is charged	0	1
	$x_{b,out}(t)$	Binary to decide when the battery is discharged	0	1
	$P_{to-grid}(t)$	Power output, electricity back to the grid (AC)	0.5 MW[a]	min(100 MW, $(0.9 \cdot E_{b,nom}/1h)$)
	$P_{to-PEM}(t)$	Power output, electricity to the electrolyzer	0.5 MW[a]	min(100 MW, $(0.9 \cdot E_{b,nom}/1h)$)
PEM-WE	$P_{grid}(t)$	Power directly from the grid/renewable plant	0.5 MW $\cdot N_{mod}$[a]	2.5 MW $\cdot N_{mod}$
	$x_{on-off}(t)$	Binary to activate or deactivate the electrolyzer	0	1
H_2 storage	$\dot{m}_{H_{2,MeOH}}(t)$	H_2 flow rate for the methanol synthesis plant	$0.2 \cdot \dot{m}_{H_{2,MeOH},nom}$	$\dot{m}_{H_{2,MeOH},nom}$

[a] 0 MW if the unit is not operating.

ANTIGONE, SCIP, and DICOPT, but their performance was worse than that of BARON.

For all the considered case studies, the annualized cost of methanol (C_{MeOH}) was minimized. In the following subsections, the optimization variables and the main constraints are discussed.

5.1. Optimization variables

The considered optimization variables can be divided into two categories: design and scheduling variables. The design variables allow defining the optimal size and capacities of the units, which mainly contribute to the investment cost, while the scheduling variables how the units are operated, thus affecting the operating costs and the production rates.

As regards the plant design, the size of the battery, electrolyzer, compression unit, H_2 storage, and methanol synthesis plant was optimized. In particular, the size of the methanol synthesis plant was estimated from the nominal H_2 input stream since a constant hydrogen conversion efficiency was assumed for the methanol plant (see Section 3.5 and [9]). This modeling choice allows reducing the number of variables seen by the optimizer, thus improving the computational performance. The nominal H_2 input stream in the methanol plant can differ from the maximum hydrogen production rate of the electrolysis unit in case there is H_2 storage. Two additional design variables that also have a high impact on the operating phase were considered, i.e., the operating pressure of the electrolysis unit and the maximum pressure ratio of the compressor. The first affects the electrolyzer efficiency as well as the size of the downstream compression unit, while the second determines the maximum pressure that can be achieved in the H_2 storage. The choice of these two design variables aims at capturing the interplay between the size of the compression unit and the H_2 storage.

A summary of the design variables and their bounds can be found in Table 4. A maximum size of 100 MW (40 modules) was considered as representative of the electrolyzer size in the short-term future [43]. The maximum size of the battery and H_2 storage was defined accordingly in order to provide a few hours of storage (around 4 h and 18 h, respectively, when the electrolyzer size is 100 MW). The electrolyzer pressure range is typical for PEM water electrolyzers. The maximum pressure ratio of the compressor unit is limited by technical issues, e.g., discharge temperature [36] and overall efficiency.

In order to calculate the optimal scheduling, optimization variables for the battery, the electrolyzer, and the H_2 storage were introduced. For the battery, the power input ($P_{in}(t)$) and the power output ($P_{to-grid}(t)$ and $P_{to-PEM}(t)$) were optimized. Additionally, two sets of binary variables ($x_{b,in}(t)$ and $x_{b,out}(t)$) were introduced to define operational constraints. Similarly, the power taken from the grid ($P_{grid}(t)$) and a binary variable ($x_{on-off}(t)$) were considered for the electrolysis unit. The hydrogen flow rate fed into the methanol synthesis plant ($\dot{m}_{H_{2,MeOH}}(t)$) determines the methanol production rate over time. The bounds of the operational variables for optimization depend on both the design optimization variables and technical constraints and will be discussed in more detail in Section 5.2.

The variables in Table 4 are shown for the more general configuration of the Power-to-Methanol plant with both storage technologies. Though the four investigated configurations (Fig. 4) could have been optimized via a single superstructure optimization problem by introducing binary variables, enumeration was preferred in order to limit the complexity of the optimization problem, which already counts 11526 variables (6 design and 11520 scheduling variables) for the flexible Power-to-Methanol plant with both storage technologies. The optimization problem was modified when considering simpler plant configurations (no storage and no flexibility) to reduce the problem size and improve convergence.

5.2. Operation constraints

The operation of the Power-to-Methanol plant depends on the size of the units and on their operational limits.

Batteries have wide operating ranges with respect to their state of charge [2]. In order to prevent deep discharge phenomena, a minimum state of charge of 10% was assumed. Some operational constraints on the hourly energy flows were also set. When active, a minimum power flow of 0.5 MW was considered in order to avoid small energy transfers, which would not be feasible for the power electronics in large plants. The maximum charge and discharge rates were also limited by either the nominal capacity of the battery or the maximum power of the electrolyzer (100 MW).

PEM water electrolyzers also have extremely wide operating limits (0%–160% relative to the nominal load [33]). However, we considered an operating range of 25%–125% since the downstream compression unit has a narrower operating range (25%–100% of the H_2 flow rate) and no buffer tank was considered between the electrolyzer and the compressor unit.

The H_2 storage located after the compression unit has a 0%–100% operating range, where 0% corresponds to the pressure inside the storage of 75 bar (no H_2 available for the methanol synthesis in the storage).

The methanol synthesis plant was assumed to always be operating over the considered time horizon within a range of 20%–100% of the nominal load [8]. This choice also allows avoiding the implementation

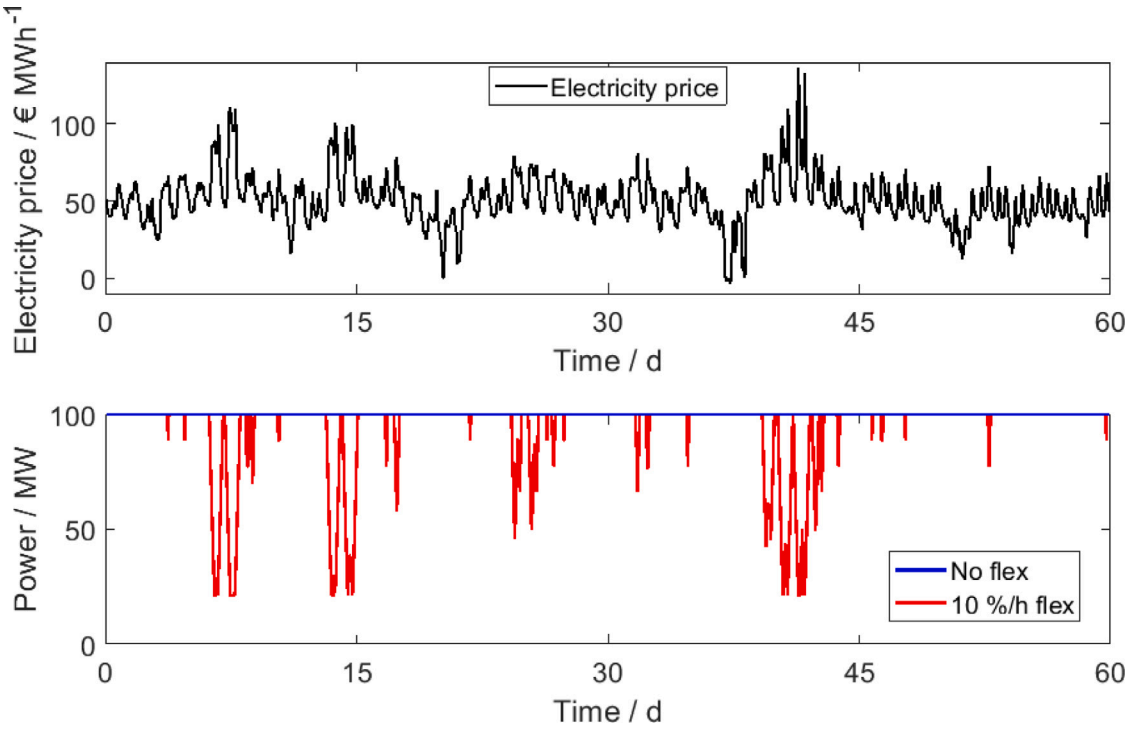

Fig. 5. Power of the PEM electrolyzer for two levels of flexibility of the methanol synthesis plant, i.e., 'No flexibility' and '10%/h flexibility'. The results are shown for the Power-to-Methanol plant without any storage for the low-price low-variable electricity price scenario (top part of the figure).

Table 5
Summary of the operation ranges of the plant units (minimum–maximum load).

Unit	Operating range
Battery	10%–100%
PEM-WE	25–125%[a]
H_2 compression	25%–100%
H_2 storage	0%–100%
Methanol synthesis plant	20%–100%

[a] Referred to the nominal load.

of additional optimization variables for the on-off, start-up and shut-down phases and the introduction of an economic penalty due to the energy and hydrogen consumption during these phases.

As mentioned in Section 5.1, the methanol flow rate is calculated from the hydrogen flow rate fed into the methanol synthesis plant ($\dot{m}_{H_{2,MeOH}}(t)$). This hydrogen flow is equal to the hydrogen flow produced by the electrolyzer unless there is the H_2 storage. In this case, the hydrogen flow to the methanol synthesis plant is considered an optimization variable. Furthermore, to investigate the effect of the flexibility of the methanol synthesis plant on its production cost, the following ramp constraint was set:

$$|\dot{m}_{H_{2,MeOH}}(t) - \dot{m}_{H_{2,MeOH}}(t-\Delta t)| \leq RL \cdot \dot{m}_{H_{2,MeOH,nom}},$$

where RL is the maximum ramp limit expressed in percentage, and $\dot{m}_{H_{2,MeOH},nom}$ is the nominal H_2 flow rate fed into the methanol synthesis plant. In case no flexibility was considered, steady-state operation at the nominal capacity of the methanol synthesis plant was assumed.

A summary of the operating limits and of the operational constraints can be found in Tables 4 and 5. We refer to the GAMS files in the Supplementary Information for the implementation of all constraints.

6. Results and discussion

In this section, the optimization results for the two case studies (grid-connected and stand-alone) are shown.

Table 6
Optimization results for the grid-connected case study without storage for the low-price low-variable electricity price scenario. Refer to Appendix A.7 for the complete results.

Flexibility %/h	Specific cost of MeOH €/kg	$MeOH_y$ kt	$CAPEX_0$ M€	$OPEX_y$ M€
0	0.91	80.3	133	51
5	0.90	76.2	133	46
10	0.90	75.7	133	46

6.1. Grid-connected case study

In order to investigate the role of storage, we compared the four plant configurations (Fig. 4) for both a low-price low-variable and a high-price highly-variable electricity profile scenarios (Fig. 2). The role of flexibility was investigated by varying the maximum ramp limit (RL) of the methanol synthesis plant (in %/h of the nominal load).

6.1.1. Low-price low-variable scenario (Historical 2021)

The calculated specific cost for methanol is around 0.9 €/kg. As shown in Table 6, the specific cost gets slightly lower (around 1%) by allowing flexible operation of the methanol synthesis plant. Since the optimal size of the methanol synthesis plant does not change by allowing flexibility in all the configurations for this electricity scenario (the electrolyzer size is at its upper bound), the cost reduction is due to the savings on the operating costs, although the overall methanol production is reduced because of the part-load operation. In fact, if the methanol synthesis plant is operated flexibly, the electrolyzer, the most energy-intense unit, can be operated at the maximum load when the electricity is cheap, and at a lower load when the electricity is expensive (Fig. 5). Nevertheless, the capacity factor of the methanol synthesis plant is above 94% (calculated on the working hours) even when the plant is operated flexibly in the considered scenario.

Storage does not improve the economic competitiveness of the plant in this scenario: the optimal solution is without any storage. The potential operating cost savings due to storage do not repay the

Table 7
Optimization results for the grid-connected case study for the high-price high-variable electricity price scenario. Only the results of the Power-to-Methanol configurations with (B&V) and without (No B&V) both storage technologies are shown here. Refer to Appendix A.7 for the complete results.

	Flexibility %/h	Specific cost of MeOH €/kg	En_{batt} MWh	V m^3	$MeOH_y$ kt	$CAPEX_0$ M€	$OPEX_y$ M€
No B&V	0	2.02	–	–	80.7	135	141
B&V	0	1.86	115	4730	47.0	196	57
No B&V	5	1.75	–	–	49.5	133	64
B&V	5	1.69	116	1210	42.4	179	43
No B&V	25	1.72	–	–	49.4	133	63
B&V	25	1.68	111	1040	42.9	177	44

investment cost for storage because of the relatively low mean value and standard deviation of the electricity price profile.

As regards the other design variables, the optimal pressure of the electrolyzer reaches the upper bound (Table A.7), which means that the increased operating costs due to the reduction of the electrolysis efficiency are lower than the additional capital cost that a bigger compression unit would have had. Also, the nominal hydrogen flow rate for the methanol synthesis plant is equal to the maximum hydrogen production of the electrolyzer since decoupling H_2 storage is not used. An optimal design solution close to the upper bounds was expected for not highly fluctuating electricity price profiles without restrictions on power availability since the cost of the plant components benefits the economy of scale.

Similar conclusions can be drawn when considering lower capital costs for the storage and electrolysis units (Scenario 2030). In fact, the relatively small fluctuations in the electricity price profile do not make storage technologies an economically viable solution, even with the reduced future costs of the storage units.

6.1.2. High-price high-variable scenario (Historical 2022)

In this scenario, the methanol cost is around two times higher than the low-price scenario, thus showing the high influence of the electricity price on the final cost of the product (Fig. 6).

Flexible operation significantly (10%–15%) reduces the methanol cost compared to the previous scenario. In particular, there is a steep decrease in the methanol cost from the 'No flexibility' and '5%/h flexibility' cases (Table 7). This result is explained by the fact that a relevant part of the hourly price variations is lower than 5% (see Appendix A.6) and by the possibility of reducing the production rate of methanol during the highly expensive electricity hours that characterize this scenario. This frequent, though optimal, operation at part loads reduces the methanol synthesis plant capacity factor to around 60% for all the configurations in this electricity price scenario. Further minor relative reductions of the cost can be noticed when higher ramp limits are allowed since the methanol production rate can adapt better to the highly fluctuating electricity price profile.

In this scenario, storage plays a relevant role, regardless of whether the methanol synthesis plant is operated constantly at nominal load or flexibly. The presence of the hydrogen vessel has the highest impact on the methanol cost since it decouples the production and the consumption of hydrogen and allows downsizing the methanol synthesis plant (7% to 40% when operating flexibly and constantly at nominal load, respectively). Thanks to the H_2 storage, the electrolyzer can be turned off during expensive electricity hours (Figs. 7 and 8), while the downstream plant is still producing methanol. Nevertheless, the optimal storage size gets lower in case the MeOH plant is operated flexibly, as already observed in literature [16,22,27]. Furthermore, the methanol synthesis plant with H_2 storage has a smoother operational profile than the case without H_2 storage (see the bottom part of Fig. 8). The battery unit also contributes to reducing the methanol cost by both supporting the electrolyzer and selling electricity back to the grid (Table A.6), thus reducing the operating costs (Fig. 6). Interestingly, more electricity can be sold to the grid during expensive electricity hours if hydrogen storage is present since the hydrogen demand of the methanol plant can still be met while the electricity stored in the battery can be sold instead of supplying it to the electrolyzer.

As regards the design of the Power-to-Methanol plant, the electrolyzer size always reaches the upper bound (see Table A.8). The nominal hydrogen flow rate into the methanol plant differs from the maximum amount of hydrogen that can be produced from the electrolyzer (around 1.9 t/h) only when there is H_2 storage. Interestingly, when there is no H_2 storage and the methanol synthesis plant is operated constantly at nominal load, more efficient production of hydrogen seems to be favored because of the high cost of electricity: The operating pressure is below the upper bound (around 31.5 bar), differently from all the other configurations.

When considering the future unit cost scenario, the methanol production cost is lower (Table A.9). Analogously to the current unit cost scenario, flexibility plays an important role in reducing the methanol production cost and the Power-to-Methanol plant with both storage technologies is still the best option (Fig. 6).

Thanks to the reduction of the installation cost of storage, bigger storage units, especially the battery, are chosen by the optimizer (Table A.9). In fact, the battery provides not only electricity to the electrolyzer but also generates high revenues by selling electricity back to the grid during expensive electricity hours (Table A.6), thus reducing significantly the overall operating costs. Due to the considered boundaries, e.g., the charging and discharging rate limits of the battery (100 MW), and the high contribution of the operating costs to the methanol production cost (Fig. 6), the optimizer chooses large-size batteries and small electrolysis and methanol synthesis. In fact, smaller electrolyzers and methanol synthesis units are less expensive and require less power, thus meaning that, during expensive electricity hours, the battery can supply electricity to the Power-to-Methanol plant and sell a large amount of the electricity to the grid generating revenues. This combined effect on CAPEX and OPEX induced by the battery effectively reduces the methanol production cost despite the reduction of the amount of produced methanol. A minimum value for the yearly methanol production was therefore set to 40 kt/y for the future unit cost scenario. This value is always obtained when batteries are present (Table A.9).

6.2. Stand-alone case study

Also in the stand-alone case study, flexible operation of the methanol synthesis plant highly affects the specific cost of methanol in both scenarios even though both storage technologies are used (Table 8). The steep reduction of the cost between the 'No flexibility' and '5% flexibility' case is mainly due to the possibility of increasing the consumption of the available electricity and thus the methanol production (see the reduction of the relative contribution of the renewable plants to the methanol production cost in Figure A.5), although the capacity factor of the methanol synthesis plant is around 60%. In both scenarios, the utilization factor of the produced electricity rises from around 65%–70% to over 90% (Figs. 9 and 10), thus reducing the renewable curtailment. Even higher utilization factors are not economically optimal since a

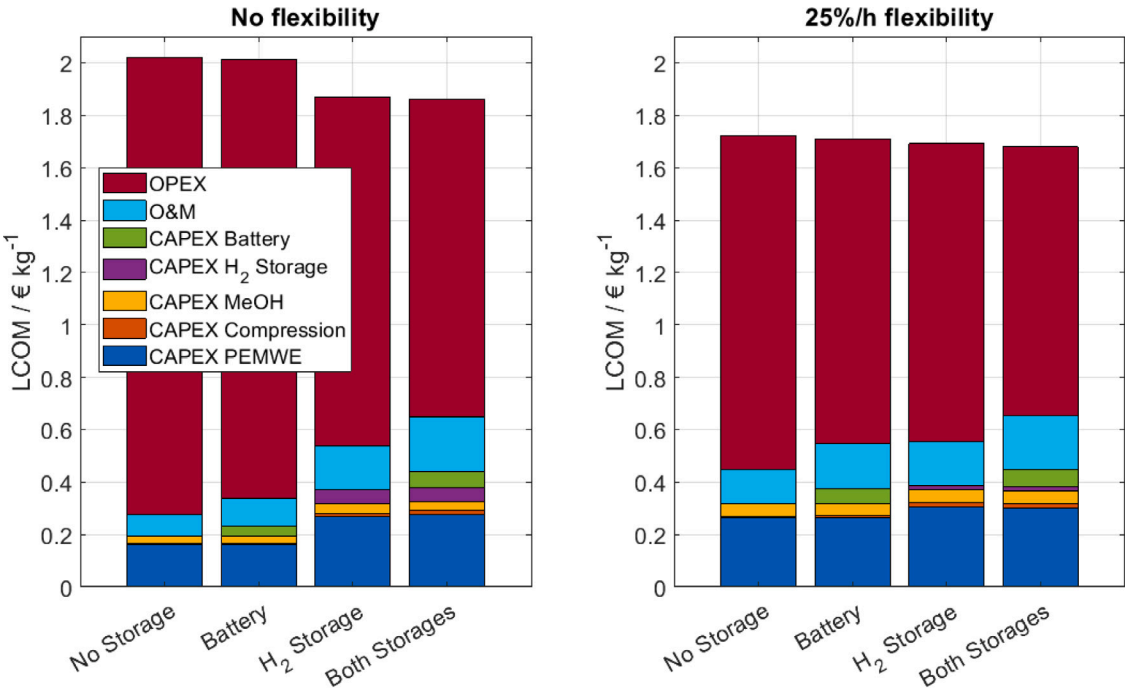

(a) **Current unit cost scenario**

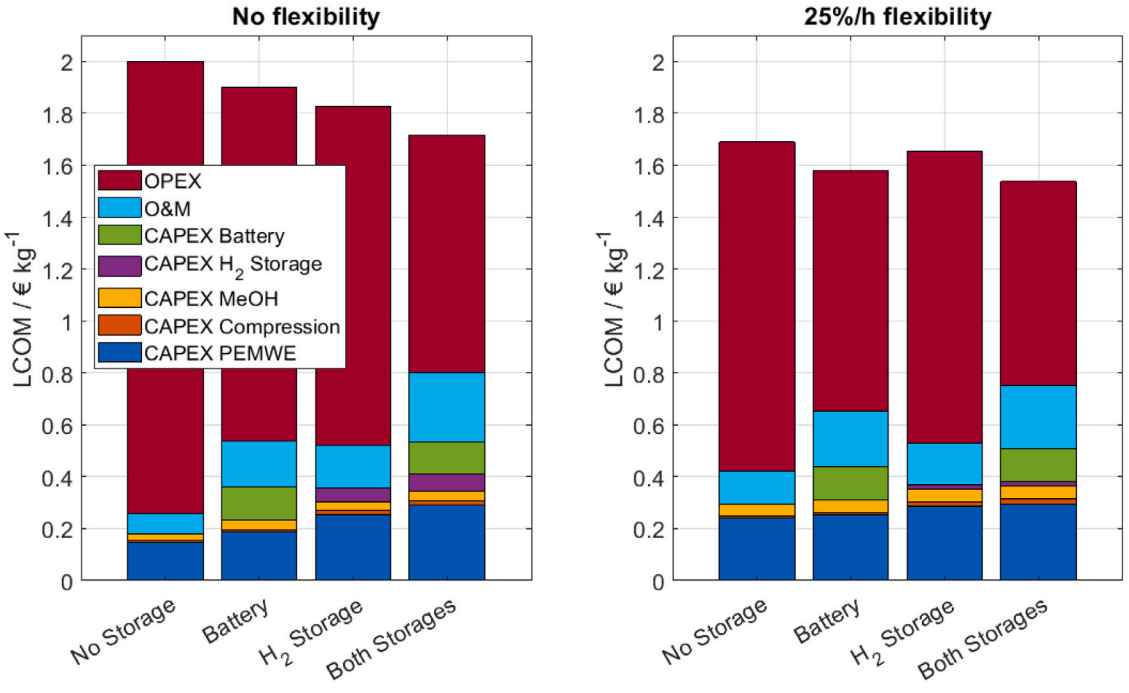

(b) **Future unit cost scenario**

Fig. 6. Relative contribution to the methanol production cost (LCOM) of the investment cost of the units and of the operating costs for the 'No flexibility' and '25 %/h flexibility' cases for 4 plant configurations, i.e., without any storage, with a battery, with a H_2 storage, and with both storage for the high-price high-variable electricity price scenario. The current and future unit cost scenarios are shown at the top and bottom of the figure, respectively.

significantly higher storage capacity would be needed to completely follow the few power peaks and its investment would not be repaid. The maximum power that the Power-to-Methanol plant can consume will therefore be lower than the installed capacity of the renewable park as already observed in other works [21,27].

Storage is essential in the stand-alone configuration to grant continuous operation of the methanol synthesis plant in both scenarios, especially in low-power production hours. H_2 storage always plays a relevant role, though its optimal volume gets lower when allowing increased flexibility: the optimizer chooses larger methanol synthesis plant sizes rather than large storage capacities (Table 8). The battery instead plays a minor role compared to the H_2 storage for the considered scenarios: the maximum amount of stored energy can satisfy the maximum power demand of the electrolyzer for less than 1 h

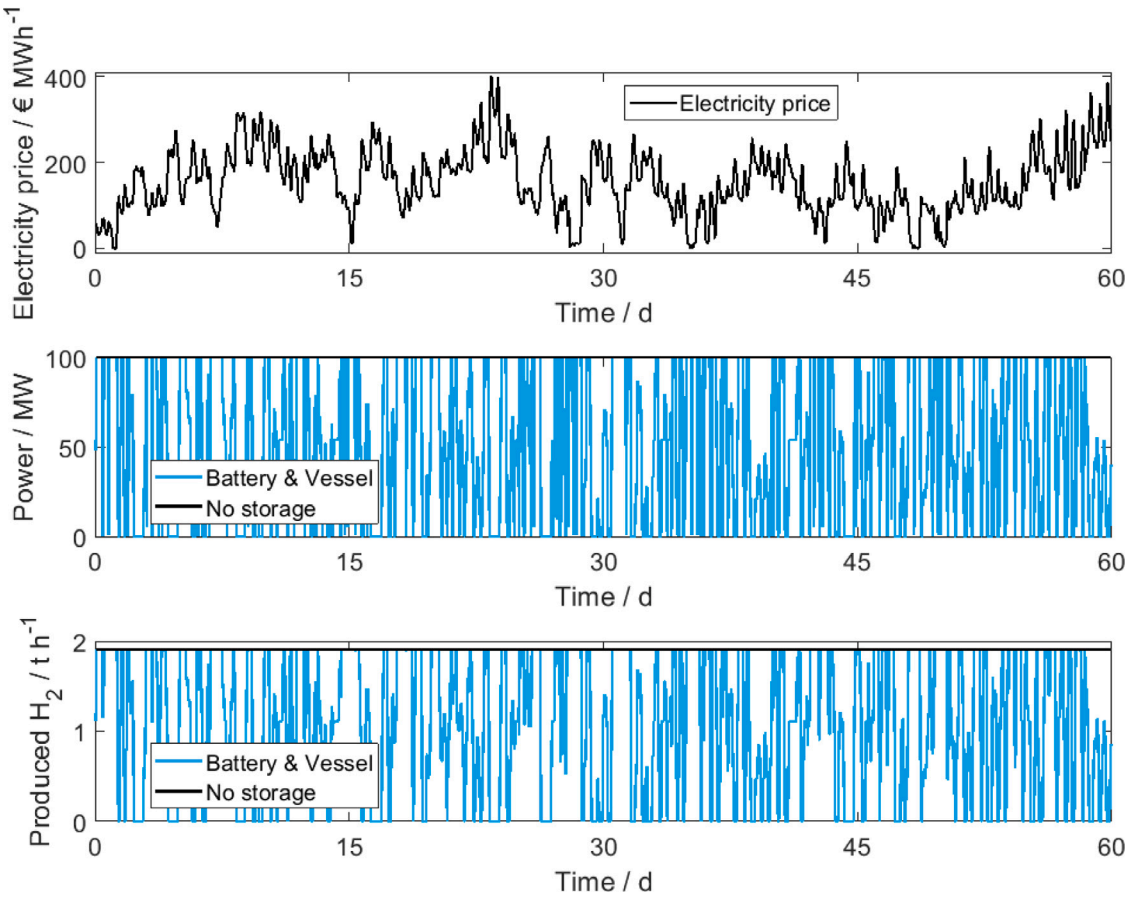

Fig. 7. Power of the PEM-WE taken from the grid over time and hydrogen produced by the electrolyzer for the 'No flexibility' case. The best ('Battery & Vessel') and worst ('No storage') cases are shown. The electricity cost profile is also shown to better interpret the optimal scheduling. Note: the power profile might not match qualitatively the hydrogen production profile for the Battery & Vessel configuration due to the additional power flowing from the battery unit.

Table 8
Optimization values for the stand-alone case study for the considered scenarios (May–Jun and Nov–Dec). Refer to Appendix A.7 for the complete results.

	Flexibility %/h	Specific cost of MeOH €/kg	En_{batt} MWh	V m^3	N_{mod} –	$\dot{m}_{H_2,MeOH,nom}$ t/h	$MeOH_y$ kt
May–Jun	0	1.78	70	5000	20	0.67	28.3
May–Jun	5	1.40	27	800	33	1.43	37.9
May–Jun	25	1.39	28	510	33	1.43	37.9
Nov–Dec	0	2.38	35	5930	15	0.46	19.5
Nov–Dec	5	1.70	23	940	28	1.22	29.2
Nov–Dec	25	1.69	17	900	26	1.15	28.5

* Bound.

(if flexibility is allowed). Nevertheless, it intensively exchanges power with the system especially during the production peaks and shortages when the electrolyzer cannot be operated (Figs. 9 and 10) and when the electrolyzer cannot be operated at full capacity (also see Figures A.6 and A.7).

When considering the future unit cost scenario, the main difference lies in the significant reduction of the methanol production cost values (9%–11%). Moreover, the methanol production cost from a flexible stand-alone Power-to-Methanol plant is significantly lower than the one from a grid-connected plant operated when electricity is expensive, e.g., in the 'high-price high-variability scenario'.

Differently from the high-price high-variability scenario of the grid-connected case study, the optimal size of both storage does not change significantly between the current and future unit cost scenarios since the battery cannot act as pure energy storage by speculating on electricity price differences. Nevertheless, a bigger battery and a relatively smaller hydrogen storage were chosen by the optimizer for the not flexible methanol plant for the May–June Scenario (Table A.10), probably because of the periodic and frequent peaks due to photovoltaic generation.

6.3. Discussion

The optimal design of the Power-to-Methanol plant with and without storage in both case studies is highly dependent on the considered scenario. Nevertheless, general trends can be observed.

6.3.1. Role of flexibility

Flexible operation turned out to be an effective way to reduce the methanol production cost in Power-to-Methanol plants both with and without storage. This is mainly due to the wide operating range of methanol synthesis plants (20%–100%), which has been shown to play a big role in methanol cost reduction for flexible stand-alone plants [28]. In fact, when the methanol plant is already operated

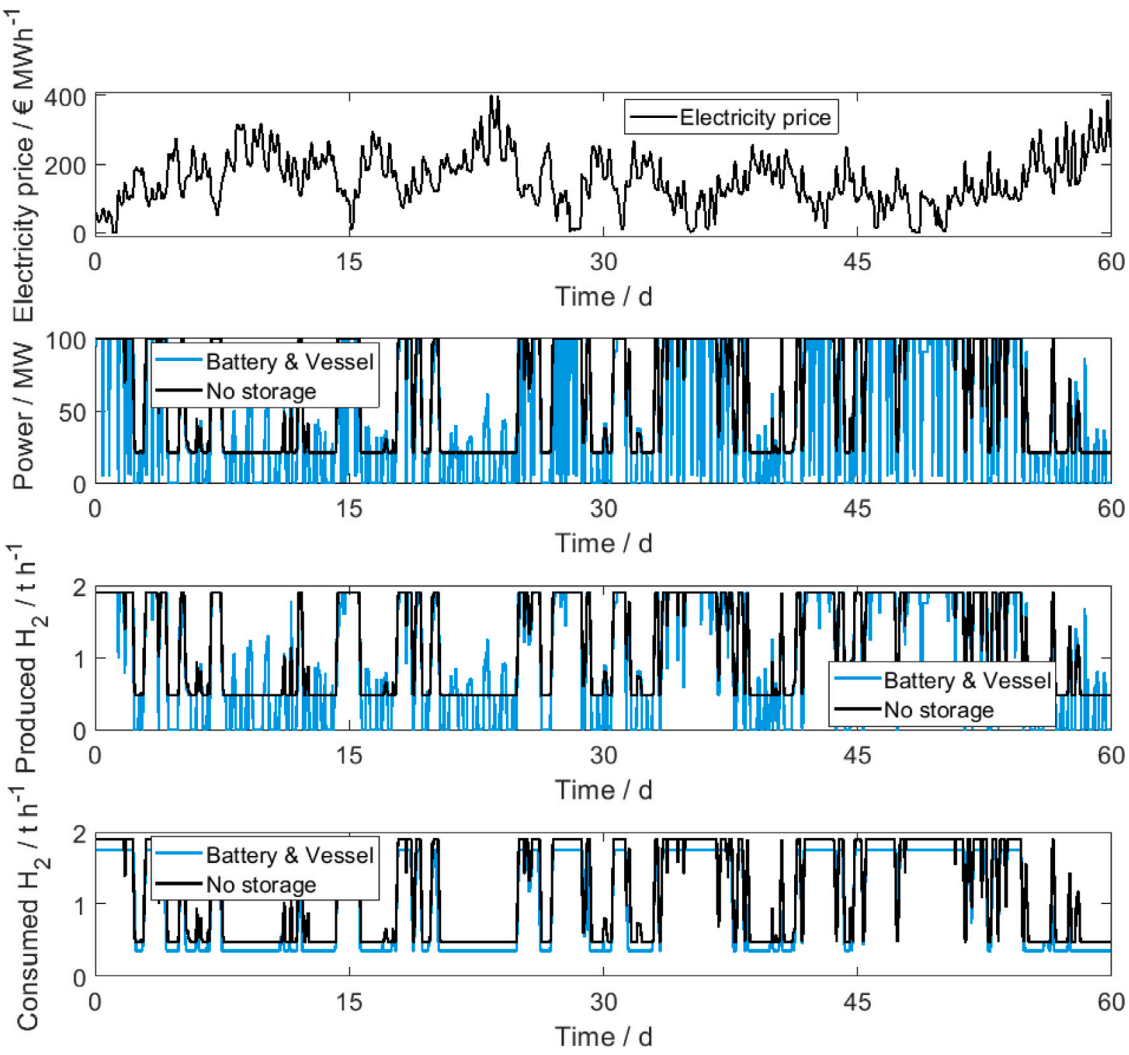

Fig. 8. Power of the PEM-WE taken from the grid and H_2 flow rate produced by the electrolyzer and consumed in the methanol synthesis plant for the '25%/h flexibility' case. The best ('Battery & Vessel') and worst ('No storage') cases are shown. The electricity cost profile is also shown to better interpret the optimal scheduling. Note: the power profile might not match qualitatively the hydrogen production profile for the Battery & Vessel configuration due to the additional power flowing from the battery unit. Also, the hydrogen production profile might not match the hydrogen consumption profile due to the hydrogen flowing from the vessel.

flexibly, the benefits obtained in our case studies by varying the ramp rate, e.g., from 10%/h to 25%/h, are lower than the reported benefits of extending the operating range of the methanol plant, e.g., from 75%–100% to 50%–100% [28], since the energy consumption can be further reduced when electricity is expensive or there is a renewable generation shortage.

The cost reduction due to the flexibility for both the grid-connected and stand-alone case studies is in line with other works in literature [21,27] even though a quantitative comparison is difficult as it depends on the considered scenarios and boundaries.

For the grid-connected case study, the reduction of the methanol production during the high-price hours allows reducing the operating costs and, at the same time, the production cost of methanol (value in agreement with the cost range calculated by IRENA (0.8–1.6 $/kg) [3]). However, the optimal capacity factor of the methanol synthesis plant highly depends on the electricity price scenario (94% and 60% for the investigated scenarios with current unit costs).

In the stand-alone case study, flexible operation allows increasing the utilization of the electricity from the renewable park and the produced methanol, thus reducing the production cost. A similar cost reduction between flexible and not flexible stand-alone Power-to-Methanol plants can be found in literature (1.50–1.85 $/kg and 1.89–2.84 $/kg for flexible and not flexible Power-to-Methanol with hydrogen storage [27]). The methanol cost reduction due to flexibility obtained by Svitnič and Sundmacher [28] was instead lower (1.39–1.58 $/kg and 1.46–1.75 $/kg for flexible and not flexible Power-to-Methanol for the renewable availability scenario including both solar and wind generation). However, this might be due to the fact that operational constraints and nonlinearities are considered in this work and that they considered a more extended process network (multiple renewable generation, storage, and hydrogen production technologies), which was able to provide relatively low production costs of methanol even when the plant was operated in steady state. The even bigger methanol production cost difference for the future unit cost scenario (0.80–1.03 $/kg in [28] vs. 1.26–2.11 €/kg in this work) can be likely explained by the different models, boundaries, and cost predictions as well as the considered technologies in the process network. Further reduction of the methanol production cost could be achieved in case some electricity is taken from another source or the plant is interfaced with the grid [26,27] since electricity can be sold (instead of curtailed) or purchased in case of renewable generation surplus and shortage, respectively.

The relative improvements in the objective function value get lower by increasing the maximum allowed ramp rate of the methanol synthesis plant. This aspect might be due to the considered time discretization since electricity price and renewable production may in practice vary

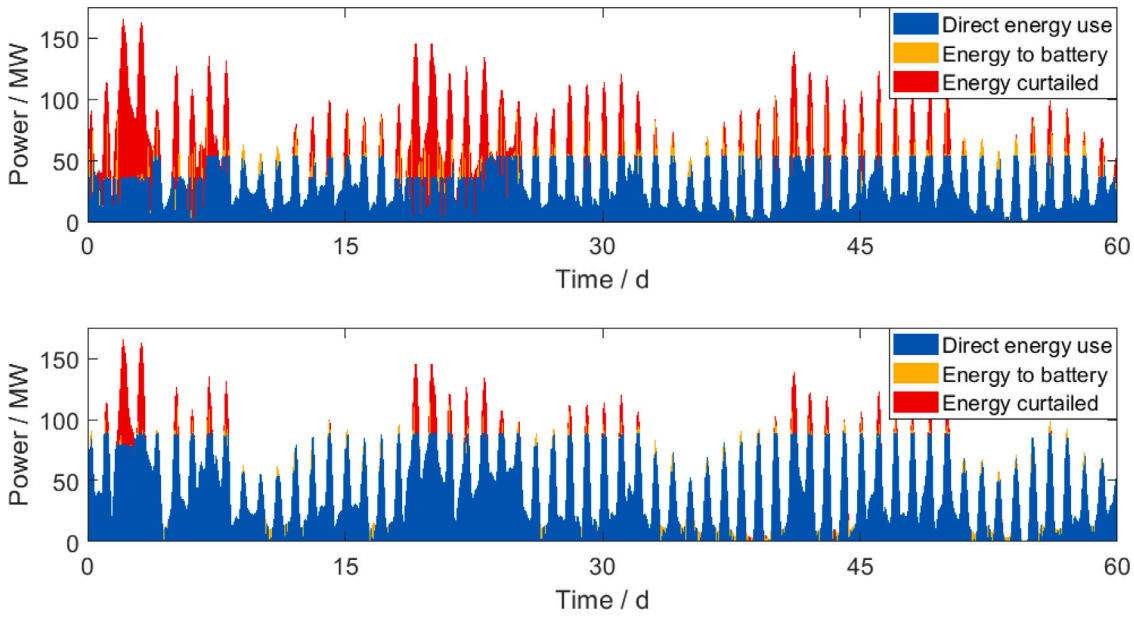

Fig. 9. Energy consumption, energy that is stored in the battery in that hour, and energy curtailed for the 'No flexibility' (top) and ± '25%/h flexibility' (bottom) cases (May–Jun scenario).

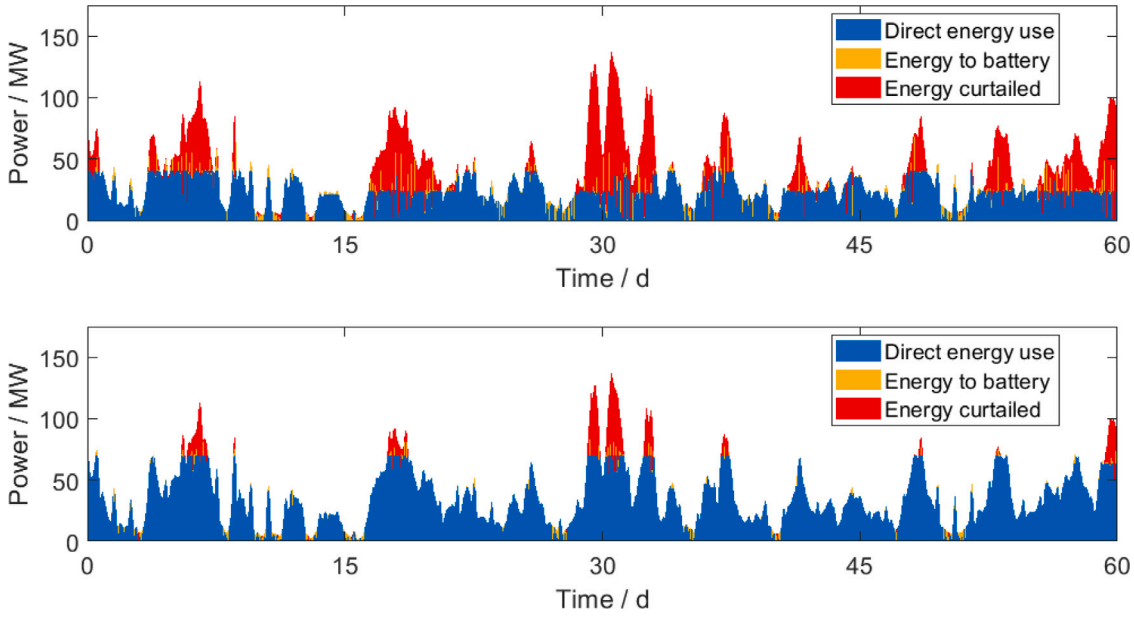

Fig. 10. Energy consumption, energy that is stored in the battery in that hour, and energy curtailed for the 'No flexibility' (top) and ± '25%/h flexibility' (bottom) cases (Nov–Dec scenario).

on a shorter time scale. Nevertheless, flexibilization raises the issue of degradation: it might be worth not carrying out extremely quick load variations if these degrade the components of the plant, e.g., the catalyst, and the related economic savings are small. The electrolyzers could particularly suffer from degradation due to frequent load changes, start-ups, and shut-downs and have a shorter operational lifetime. However, these phenomena are still not well understood and are difficult to model. An additional over-sizing of the electrolyzer to consider the long-term efficiency loss [51] or considering different operating strategies, e.g., avoiding frequent start-ups and shut-downs by introducing a penalty function, could be alternative ways to take into account these phenomena and refine the results. The possibility of shutting down the methanol plant (not considered in this work) could instead be beneficial [12] in case the economic penalty due to degradation and start-ups/shut-downs procedures is not too high, since it might reduce the optimal size and cost of storage.

6.3.2. Role of storage

The role of storage depends on the considered boundaries, especially when the plant purchases electricity from the grid. When the electricity is cheap and its profile is not highly fluctuating as in the historical scenario 2021, the savings that the storage could allow are not sufficient to repay the investment. If the electricity price is higher as in the historical scenario 2022, storage improves the economic profitability of the plant. Nevertheless, flexibilization of the methanol synthesis plant has a greater economic benefit compared to adding storage.

For the considered boundary conditions and the current unit cost scenario, the H_2 vessel provides big economic savings. The potential of the H_2 vessel estimated in this optimization problem could even be rather conservative. In fact, a hydrogen bypass could be applied when the hydrogen consumption of the methanol synthesis plant is higher than the produced hydrogen ($\dot{m}_{H_2,MeOH}(t) \geq \dot{m}_{H_2,prod}(t)$): the produced hydrogen is compressed and directly fed into the methanol synthesis plant together with the already pressurized hydrogen taken from the

vessel. The bypass would save electricity in the compression unit since the produced hydrogen has to be compressed up to the pressure of the synthesis plant (75 bar) instead of the higher pressure inside the vessel. From a post-analysis of the worst case (not flexible Power-to-Methanol plant with H_2 storage for the high-price high-variability scenario), the estimated economic savings of a bypass would be around 9% of the operating costs of the compression unit, but less than 0.1% of the overall yearly operating costs. However, modeling this configuration would have introduced additional variables and complexity to the optimization problem for a little improvement. Therefore, it was not considered in this work.

Compared to the vessel, the benefit of battery on the production cost is lower for the current unit cost scenario and the considered boundary conditions despite the nearly ideal model; in fact, small capacities are chosen by the optimizer. In the future unit cost scenario instead, batteries become competitive and can effectively reduce the methanol production cost when the electricity price is highly variable. In any case, batteries play an essential role in stand-alone configurations to supply electricity in case of shortage and to damp power production fluctuations with a time scale lower than one hour (considered time step). Also, the battery is used for short-term storage (a few hours). For longer storage periods, the H_2 vessel seems to be a better option since it does not suffer from self-discharge. Nevertheless, the potential of batteries could change when considering other battery types [28] or boundary conditions.

6.3.3. Challenges and opportunities for grid-connected Power-to-Methanol plants

In this work, no constraints related to grid congestions were considered in the grid-connected case study, since it would have required the choice of the location of the Power-to-Methanol plant and a dedicated model of the grid [52], which was out of the scope. Nevertheless, its consideration could have probably affected the optimization results since bigger batteries could supply energy to the Power-to-Methanol plant even in case of grid congestion.

Furthermore, a different optimal design of the Power-to-Methanol plant would probably have been obtained by considering not only the participation in the day-ahead market but also in the ancillary service market with both the battery and the water electrolysis units (PEM water electrolyzers can offer up to primary reserve [35], and the provision of ancillary services can reduce the hydrogen production cost [35,53]): part of the capacity in MW of both units could be reserved to help balancing the electricity grid for economic compensation. In fact, bidding simultaneously in multiple markets has been shown to offer relevant savings in operating costs [54,55]. In this case, the Power-to-Methanol configuration with both storage technologies (Fig. 1) would most likely be favored since it allows acting on these markets without necessarily having a direct effect on methanol production thanks to the buffer hydrogen vessel, which could damp quick hydrogen production fluctuations related to grid reserve operation. The additional revenues could make batteries more competitive, thus increasing their optimal installed capacity, and might increase the oversize of the electrolysis unit compared to the methanol synthesis plant or the size of the hydrogen vessel since the electrolyzer would not be operated at its maximum load.

6.3.4. Scenario-dependency

In this work, the role of storage and flexibility was analyzed for a few rather different historical electricity price and renewable generation scenarios. Nevertheless, other scenarios could be investigated by using the GAMS code provided with the Supplementary Information since it was shown that the considered scenarios and boundaries can significantly affect the optimal design of the plant. If there is no certainty about the scenarios, multiple scenarios could be considered in a two-stage stochastic design and scheduling optimization problem. Also, the design of the plant for the stand-alone case study could be optimized over longer time frames to better account for the seasonal behavior of renewable generation, especially when there is no complementarity of renewable power production throughout the year. However, reformulations of the optimization problem or time aggregation series techniques [47] should be used to reduce the computational burden.

7. Conclusions

A combined design and scheduling optimization problem was formulated in GAMS for a Power-to-Methanol plant with both a battery and a hydrogen vessel to investigate the role of flexibility and storage. This problem was solved with the optimizer BARON for a grid-connected and stand-alone case study for different electricity price and renewable generation profiles and unit cost scenarios.

Although overall global optimality cannot be guaranteed, the results suggest that flexible operation of the entire Power-to-Methanol plant significantly reduces the production cost of methanol in every case study. Also, it was noted that no significant cost reduction was achieved by considering maximum ramp rates higher than 10%/h for the considered scenarios and time discretization.

In the grid-connected case study, storage technologies play a relevant role when the electricity profile is highly fluctuating and at a high average price. In this scenario, the Power-to-Methanol configuration with both the battery and the H_2 storage minimizes the methanol production cost. However, among these two storage technologies, the H_2 storage provides the major economic benefits since it allows the decoupling between hydrogen production and conversion and thus a downsizing of the methanol synthesis plant. In the stand-alone case study, storage is essential in all the scenarios, and it is widely used regardless of whether the methanol synthesis plant is operated constantly at nominal load or flexibly.

When considering future (2030) unit cost reductions of the key technologies, i.e., batteries, hydrogen storage, and electrolyzers, batteries could be highly beneficial to reduce the production cost of methanol in grid-connected plants with highly fluctuating price profiles since they can both provide electricity to the Power-to-Methanol plant and generate high revenues by selling electricity to the grid during expensive electricity hours.

Furthermore, it must be mentioned that longer time series should be considered for the optimal plant design to account for renewable production seasonality since the optimal designs differ when considering different generation scenarios. However, some time-aggregation series techniques [28,47], multi-period optimization [56], or problem reformulations should be applied to numerically handle these optimization problems [30]. Finally, some models of the units could be improved, e.g., by considering operating maps or degradation phenomena in the electrolyzer due to flexible operation, to increase the accuracy of the results. Also, extending the model to include other storage technologies [28] and the participation in the ancillary service market for the optimal design of grid-connected Power-to-Methanol plants could shed light on the full potential of storage. Moreover, the built optimization framework can be adapted to test other electricity price and renewable power profiles, other configurations, e.g., with the hydrogen bypass, or used for other Power-to-X processes by adjusting the key parameters.

CRediT authorship contribution statement

Simone Mucci: Conceptualization, Methodology, Software, Investigation, Visualization, Writing – original draft. **Alexander Mitsos:** Conceptualization, Methodology, Supervision, Writing – review & editing, Funding acquisition. **Dominik Bongartz:** Conceptualization, Methodology, Supervision, Writing – review & editing, Funding acquisition, Project administration.

Declaration of competing interest

The authors declare that they have no known competing financial interests or personal relationships that could have appeared to influence the work reported in this paper.

Data availability

Data and code are made available as Supplementary Information.

Acknowledgments

The authors gratefully acknowledge the financial support by the German Federal Ministry of Education and Research (BMBF) within the H2Giga project DERIEL (grant number 03HY122D). The authors would also like to thank Dominik P. Goldstein for the creation of a submodel inserted in the Aspen Plus flowsheet of the methanol synthesis plant.

Appendix

A.1. PEM water electrolyzer efficiency

The implemented efficiency law of the PEM water electrolyzer (η_{PEM}) is a function of the power of the electrolysis module (P_{mod}) and the operating pressure p_{PEM}, and it is defined as follows:

$$\eta_{PEM} = a_{00} + a_{10} \cdot P_{mod} + a_{20} \cdot P_{mod}^2 + a_{01} \cdot p_{PEM},$$

where P_{mod} is equal to the overall power of the electrolyzer P_{PEM} divided by the number of modules (N_{mod}).

The values of the parameters were obtained by fitting the results of the electrolyzer model [42] in the power and pressure ranges of 0.2–2.5 MW and 20-40 bar, respectively, and are collected in Table A.1. A graphical representation of the efficiency is shown in Figure A.1.

Table A.1
Parameters for the efficiency law of the electrolyzer (R^2=0.999).

	Values	Unit
a_{00}	0.813	–
a_{10}	$-1.010 \cdot 10^{-01}$	MW^{-1}
a_{20}	$+1.397 \cdot 10^{-02}$	MW^{-2}
a_{01}	$-3.118 \cdot 10^{-04}$	bar^{-1}

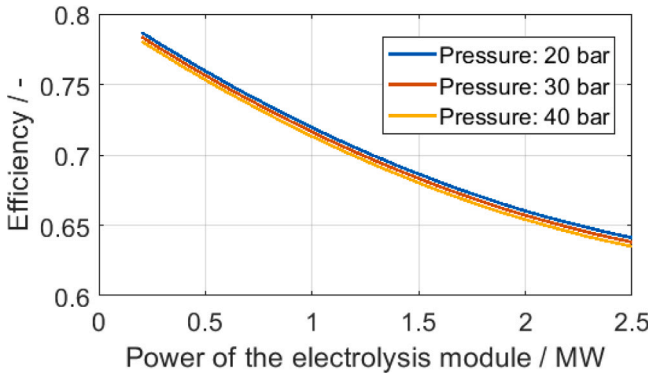

Fig. A.1. Electrolyzer efficiency with respect to the power of an electrolysis module for three pressures.

A.2. Thermophysical properties

The thermophysical properties of hydrogen from the Aspen database (Peng–Robinson property method) were used to estimate the parameters of c_p and k, and as the benchmark for the model results.

Table A.2 shows the comparison between the calculated power of the compressor unit and the Aspen Plus data for a hydrogen inlet stream of 1900 kg/h at 40 bar for different pressure ratios (β). The error for the considered operating points is lower than 1%.

Table A.2
Compressor model validation.

β	Model	Aspen data
2.0	710 kW	710 kW
2.5	970 kW	973 kW
3.0	1196 kW	1202 kW
3.5	1397 kW	1406 kW

In Figure A.2, the density of hydrogen at high pressure and its linear approximation for the hydrogen storage model is shown.

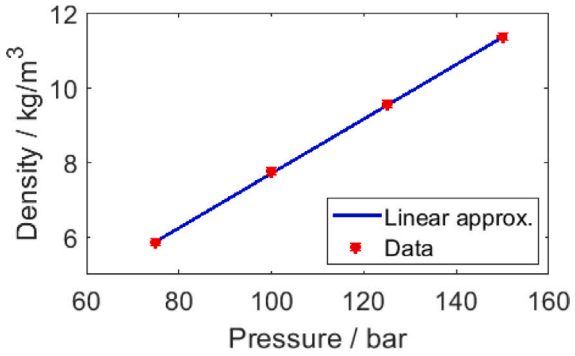

Fig. A.2. H_2 density at 25 °C as function of the pressure (data from the Aspen database).

A.3. Hydrogen storage cost

The considered hydrogen storage cost is 500 $/kg, which corresponds to the target cost for 160-bar stationary gaseous hydrogen tanks for the year 2020 [57]. This value was converted from the specific cost for unit of hydrogen mass into the specific cost for unit of volume and updated from year 2007 to year 2021 as follows:

$$\text{Cost}_{\text{vessel}} = 500 \ \frac{\$}{\text{kg}} \cdot 0.073 \ \frac{\text{kg}}{\text{m}^3\text{bar}} \cdot (160 \text{ bar} - 1 \text{ bar}) \cdot \text{UF},$$

where $0.073 \ \frac{\text{kg}}{\text{m}^3\text{bar}} \cdot (160 \text{ bar} - 1 \text{ bar})$ determines the available hydrogen mass content per unit of volume, and UF is the update factor equal to 1.35. The calculated cost is around 7800 $/m^3. Lower specific costs for vessels might be possible in scenarios with higher production volumes [57] and considering a lower maximum pressure inside the vessel, which reduces the wall thickness, thus the material cost.

A.4. Methanol synthesis plant

The plant was modeled in Aspen Plus® V11 (Fig. A.3). The property methods *PSRK* and *NRTL* were used for the thermodynamic properties in high and low pressure units, respectively. The methanol synthesis occurs in a two-stage multi-tubular reactor, which is cooled via evaporating water at around 245 °C. The operating pressure of the reactor unit is around 75 bar, and a 1 bar pressure drop was assumed for each reactor stage. A commercial catalyst $Cu/ZnO/Al_2O_3$ is considered for the implemented kinetic model LHHW (Langmuir Hinshelwood Hougen Watson) [58,59]. The choice of having two reactor stages is motivated by the low conversion per pass. The intermediate removal of products via condensation helps shift the chemical equilibrium.

After the second stage of the reactor, the unreacted gases are separated from crude methanol, the mixture of water and methanol, via condensation and partially (98%) recycled back to the reactor. Also, a membrane separation process [60] was considered to partially (90%) recover H_2 from the purge stream.

Crude methanol is then purified via distillation to meet the desired purity specification, i.e., 99.85%wt. (AA grade methanol). Heat for

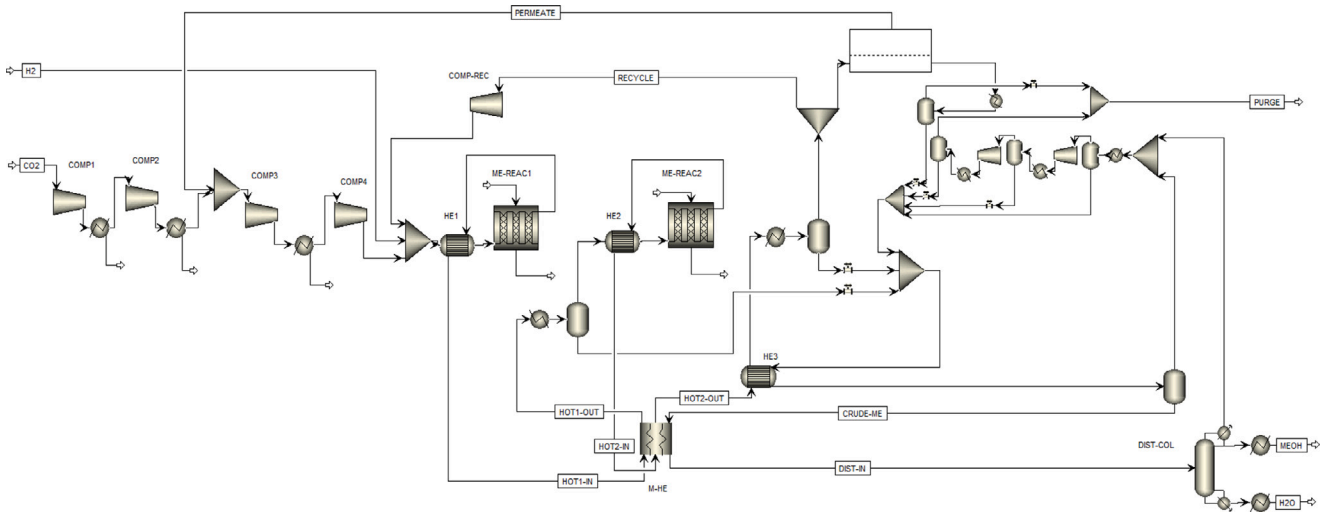

Fig. A.3. Methanol synthesis plant model in Aspen Plus® V11.

Table A.3
Main data of the reference methanol synthesis plant.

	Values
H_2 mass flow rate	1.9 t/h
CO_2 mass flow rate	15.4 t/h
CH_3OH mass flow rate	9.9 t/h
Overall electricity demand	1.8 MW
Overall cooling demand	13.8 MW
Net heat demand	0 MW
First law efficiency	84.3%

Table A.4
Percentage of the hourly price or renewable power availability variations between consecutive hours lower than 5%, 10%, and 25% for the considered scenarios. The relative hourly variations were calculated with respect to the average value over the considered scenario, i.e., 51 €/MWh, 154 €/MWh, 52 MW, and 39 MW for the 'Historical 2021', 'Historical 2022', 'May–Jun', and 'Nov–Dec' scenarios, respectively.

Hourly variations	Historical 2021	Historical 2022	May–Jun	Nov–Dec
≤ 5%	48%	42%	36%	52%
≤ 10%	72%	63%	50%	75%
≤ 25%	96%	93%	80%	97%

the reboiler can be supplied via heat integration. In particular, the surplus heat of the methanol reactor and the heat from the purge stream combustion are sufficient to satisfy its thermal demand. However, this heat integration is not shown in the flowsheet in Figure A.3, though it was considered for the calculation of the heat and cooling demands.

Table A.3 summarizes the key information about the methanol synthesis plant that was used as the reference for the technical and economical analysis.

A.5. Methanol synthesis plant cost

The CAPEX of the main equipment units of the methanol synthesis plant (Fig. A.3), i.e., compressors, reactor, heat exchangers, flashes, and distillation column, was estimated by using the cost models proposed by Biegler et al. [46]. The cost of the membrane was estimated according to Ramírez-Santos et al.'s model [60].

Biegler et al.'s method [46] is based on the well-established Guthrie's method [61], which estimates the bare module cost of the equipment with accuracy within the range of ± 25%–40%. A multiplying factor of 1.85 [46] was then used to account for fixed and working capital costs. An update factor from 1968 to 2021 of 6.15 was considered.

The estimated CAPEX of the reference methanol synthesis plant with a yearly production of 0.08 Mt is 27.8 M€ (350 €/(t/y)). This value is within the typical range for large-scale methanol synthesis plants (200–700 $/(t/y) [62]), which means that the capital cost is probably underestimated. On a similar production capacity (0.06 Mt/y), the estimated investment cost of a small-scale methanol synthesis plant in Texas was around 40 M$ [62]. The difference might be due to the uncertainty of the cost models and the different boundary conditions (the steam methane reforming and hydrogen compression units are also included in the plant in Texas). The estimated investment cost is in line with an e-methanol plant in Norway (yearly production of 0.1 Mt and a capital cost of 200 M$ [3]) if the cost of the electrolysis unit and its replacement after 10 years are considered.

Table A.5
Assumed capital cost values of the key units for the base case and future unit cost scenarios (values referred to the year 2021).

	Base case (2021)	Scenario 2030
Battery	368 $/kWh [32]	214 $/kWh [32]
Electrolyzer	Correlation[a] [43]	Correlation[a] [43]
Hydrogen storage	7800 $/m^3 [57]	7020 $/m^3 [57]
PV	857 $/kW [50]	690[b] $/kW [63]
Wind onshore	1325 $/kW [50]	1260[b] $/kW [64]

[a] It depends on the installation year.

[b] Average value of the extremes of the predicted range.

Table A.6
Optimization results for the grid-connected case study for the high-price high-variable electricity price scenario for the plant configurations with battery, i.e., with battery (B) and with both storage (B&V) for the current and future unit cost scenario: Utilization of the energy stored in the battery. Note: the tabled yearly revenue obtained by selling the electricity to the grid does not account for the purchase of the electricity.

	Flexibility %/h	Yearly energy to PEM-WE GWh	Yearly energy to the grid GWh	Yearly revenue for the electricity sell M€
B	0	83.1	0.1	0
B&V	0	26.9	54.3	11.9
B	25	49.3	34.6	8.2
B&V	25	31.1	49.8	11.5
Future unit cost scenario				
B	0	95.3	88.8	17.6
B&V	0	33.0	150.7	32.2
B	25	72.1	110.2	25.0
B&V	25	48.5	134.9	30.6

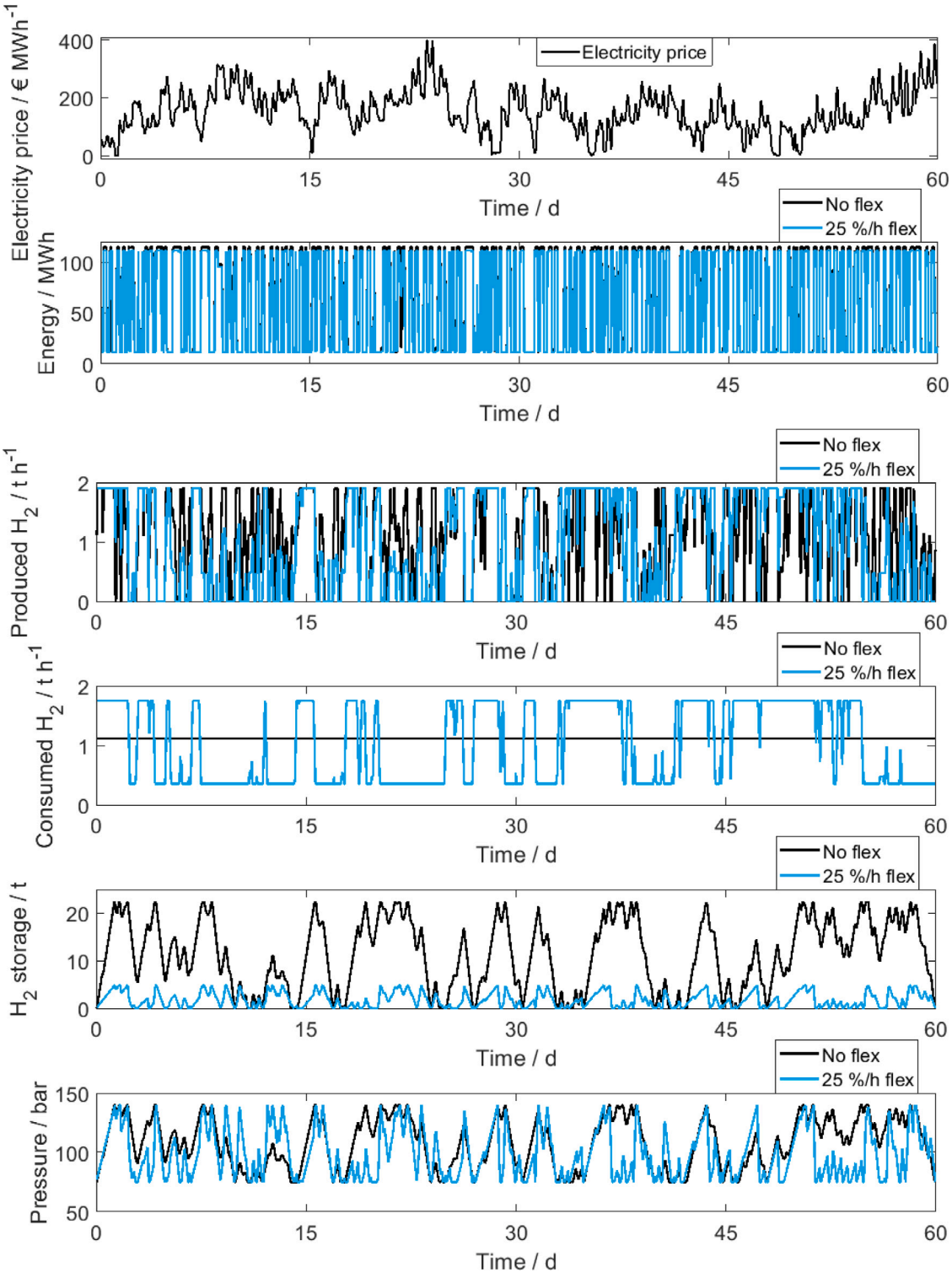

Fig. A.4. Energy content of the battery, H_2 produced by the electrolyzer, H_2 consumed in the methanol plant, and H_2 content and pressure inside the H_2 vessel for the 'No flexibility' and '25%/h flexibility' cases for the current unit cost scenario. Only the results of the 'Battery & Vessel' configuration are shown. The electricity cost profile is also shown to better interpret the optimal scheduling. Note: the energy profiles of the battery for the 'No flexibility' and '25%/h flexibility' cases are similar, thus they can hardly be distinguished in the picture.

A.6. Scenarios

In this section, additional details about the electricity price, renewable availability, and unit cost scenarios are shown.

Table A.4 shows that a relevant part of the hourly variations of the electricity price and renewable power availability profiles (relative to the mean value over the considered scenario) are lower than 5%. This explains why moderate flexibility of the methanol synthesis plant

Table A.7
Optimization results for the grid-connected case study for the low-price low-variable electricity price scenario for the 4 plant configurations, i.e., with both storage (B&V), with the hydrogen vessel (V), with battery (B), and without any storage (No B&V).

	Flexibility	Specific cost of MeOH	En_{batt}	V	N_{mod}	p_{PEM}	β_{max}	$\dot{m}_{H_2,MeOH,nom}$	$MeOH_y$	$CAPEX_0$	$OPEX_y$
	%/h	€/kg	MWh	m^3	–	bar	–	t/h	kt	M€	M€
No B&V	0	0.91	–	–	40[a]	40[a]	1.88[a]	1.91	80.3	133	51
B	0	0.91	5[a]	–	40[a]	40[a]	1.88[a]	1.91	80.3	134	51
V	0	0.91	–	25[a]	40[a]	40[a]	1.88[a]	1.91	80.3	133	51
B&V	0	0.91	5[a]	25[a]	40[a]	40[a]	1.88[a]	1.91	80.3	135	51
No B&V	5	0.90	–	–	40[a]	40[a]	1.88[a]	1.91	76.2	133	46
B	5	0.91	5[a]	–	40[a]	40[a]	1.88[a]	1.91	76.3	134	46
V	5	0.90	–	25[a]	40[a]	40[a]	1.88[a]	1.91	76.2	133	46
B&V	5	0.90	5[a]	25[a]	40[a]	40[a]	1.88[a]	1.91	76.3	135	46
No B&V	10	0.90	–	–	40[a]	40[a]	1.88[a]	1.91	75.7	133	46
B	10	0.90	5[a]	–	40[a]	40[a]	1.88[a]	1.91	75.7	134	46
V	10	0.90	–	25[a]	40[a]	40[a]	1.88[a]	1.91	75.7	133	46
B&V	10	0.90	5[a]	25[a]	40[a]	40[a]	1.88[a]	1.91	75.7	135	46

[a] Bound.

Table A.8
Optimization results for the grid-connected case study for the high-price high-variable electricity price scenario for the 4 plant configurations, i.e., with both storage (B&V), with the hydrogen vessel (V), with battery (B), and without any storage (No B&V).

	Flexibility	Specific cost of MeOH	En_{batt}	V	N_{mod}	p_{PEM}	β_{max}	$\dot{m}_{H_2,MeOH,nom}$	$MeOH_y$	$CAPEX_0$	$OPEX_y$
	%/h	€/kg	MWh	m^3	–	bar	–	t/h	kt	M€	M€
No B&V	0	2.02	–	–	40[a]	31.5	2.38	1.91	80.7	135	141
B	0	2.01	116	–	40[a]	31.6	2.38	1.91	80.7	171	135
V	0	1.88	–	4940	40[a]	40[a]	3.5[a]	1.15	48.5	162	65
B&V	0	1.86	115	4730	40[a]	40[a]	3.5[a]	1.11	47.0	196	57
No B&V	5	1.75	–	–	40[a]	40[a]	1.88[a]	1.91	49.5	133	64
B	5	1.74	115	–	40[a]	40[a]	1.88[a]	1.91	49.2	169	59
V	5	1.70	–	1320	40[a]	40[a]	3.5[a]	1.74	42.7	144	49
B&V	5	1.69	116	1210	40[a]	40[a]	3.5[a]	1.74	42.9	180	44
No B&V	10	1.73	–	–	40[a]	40[a]	1.88[a]	1.91	49.5	133	64
B	10	1.72	111	–	40[a]	40[a]	1.88[a]	1.91	49.3	168	58
V	10	1.69	–	1250	40[a]	40[a]	3.5[a]	1.74	42.7	144	49
B&V	10	1.68	116	1130	40[a]	40[a]	3.5[a]	1.74	42.4	179	43
No B&V	25	1.72	–	–	40[a]	40[a]	1.88[a]	1.91	49.4	133	63
B	25	1.71	115	–	40[a]	40[a]	1.88[a]	1.91	49.3	169	57
V	25	1.69	–	1100	40[a]	40[a]	3.5[a]	1.74	42.7	143	49
B&V	25	1.68	111	1040	40[a]	40[a]	3.5[a]	1.75	42.9	177	44

[a] Bound.

(in %/h) is already highly beneficial from an economic perspective. However, a linear correlation between the variability of the scenarios and the flexibility of the methanol synthesis plant cannot be established since other factors, e.g., storage utilization, operating constraints, and chosen objective function play a role.

To investigate the effect of the capital cost of the units on the optimal solution, future unit cost predictions were considered. In particular, the combined design and scheduling optimization problems were solved by assuming capital cost predictions for the year 2030 (Scenario 2030) and considering the same electricity price and renewable availability profiles. A reduction in the investment cost of the battery, electrolyzer, hydrogen storage, photovoltaic and wind power plants was considered (see Table A.5). The investment cost for the compression and methanol synthesis unit was instead assumed constant since no significant learning rate is expected.

A.7. Optimization results

In this section, additional optimization results are provided.

A.7.1. Grid-connected case study

The optimal design variables and the key performance metrics for the two electricity price scenarios of the grid-connected case study are shown in Tables A.7, A.8, and A.9. For the low-price low-variability scenario, the optimization results for the future unit cost scenario are not shown since they differ only slightly from the ones already shown in Table A.7: the production cost of methanol is slightly lower (0.88–0.89 €/kg) due to the reduction of the investment cost for the electrolysis unit.

Figure A.4 shows how the battery and the H_2 storage are optimally operated in the high-price high-variable electricity scenario (the produced and consumed hydrogen flow rates are also shown to better interpret the operation of the H_2 storage). As expected, the energy stored in the battery and the hydrogen in the vessel are consumed within a few days, thus confirming that the chosen time frame for scheduling (2 months) is suitable. While the use of the battery is similar between the 'No flexibility' and '25%/h flexibility' cases both qualitatively (Fig. A.4) and quantitatively (Table A.6), major differences can be noticed in the H_2 storage. The amount of hydrogen stored inside the vessel is significantly lower when the methanol synthesis plant is operated flexibly. A similar qualitative behavior can instead be noticed in the pressure profile (dependent on both the amount of hydrogen and the storage volume). The differences could be explained by the different optimal operating strategies.

A.7.2. Stand-alone case study

The contribution of the process units to the methanol production cost, the optimal design variables, and the key performance metrics for the two power availability scenarios of the stand-alone case study are shown in Figure A.5 and Table A.10. Despite considering two extremely

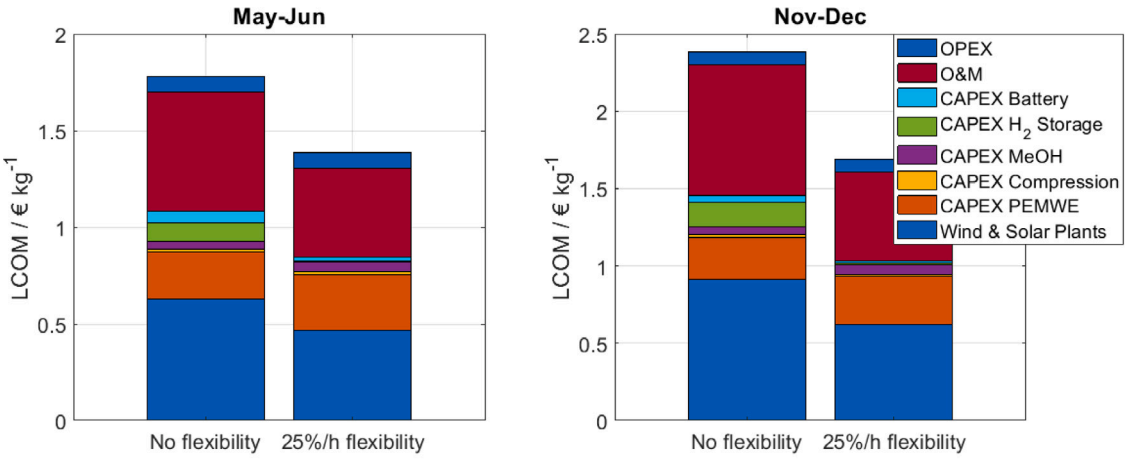

(a) **Current unit cost scenario**

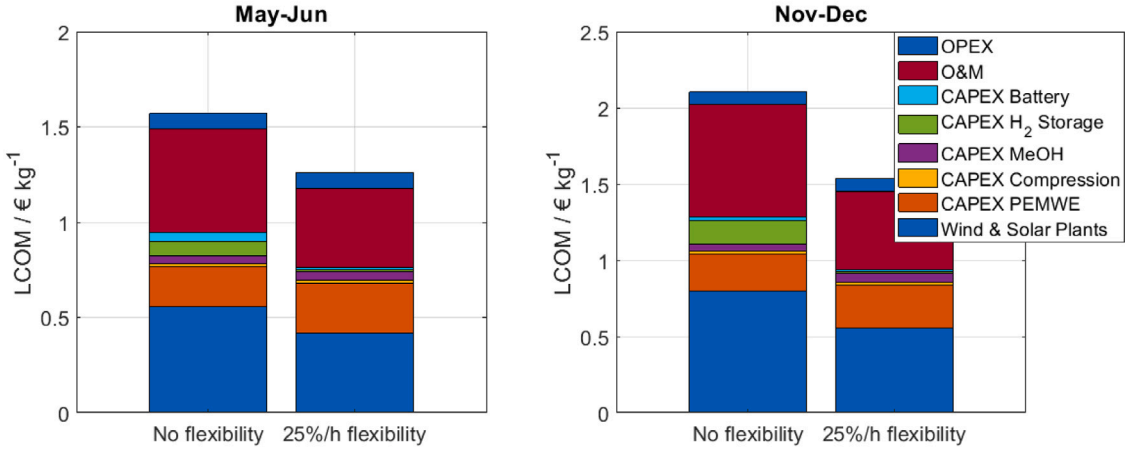

(b) **Future unit cost scenario**

Fig. A.5. Relative contribution to the methanol production cost (LCOM) of the investment cost of the units and of the operating costs for the 'No flexibility' and '25%/h flexibility' cases for the 'May–Jun' and 'Nov–Dec' scenarios. The current and future unit cost scenarios are shown at the top and bottom of the figure, respectively.
Note: the high share of O&M in the methanol production cost is due to the fact that the O&M expenditures of the renewable generation park are included.

Table A.9
Optimization results for the grid-connected case study for the high-price high-variable electricity price scenario with the reduced investment costs (Scenario 2030) for the 4 plant configurations, i.e., with both storage (B&V), with the hydrogen vessel (V), with battery (B), and without any storage (No B&V).

	Flexibility	Specific cost of MeOH	En_{batt}	V	N_{mod}	p_{PEM}	β_{max}	$\dot{m}_{H_{2,MeOH},nom}$	$MeOH_y$	$CAPEX_0$	$OPEX_y$
	%/h	€/kg	MWh	m^3	–	bar	–	t/h	kt	M€	M€
No B&V	0	2.00	–	–	40[a]	31.7	2.36	1.91	80.6	126	140
B	0	1.90	347	–	25	37.5	2.00	0.95	40.0	143	54
V	0	1.83	–	5430	40[a]	40[a]	1.88[a]	1.11	46.8	153	61
B&V	0	1.72	347	5470	39	40[a]	1.88[a]	0.95	40.0	212	37
No B&V	5	1.72	–	–	40[a]	40[a]	1.88[a]	1.91	48.7	124	63
B	5	1.62	347	–	33	40[a]	1.88[a]	1.57	40.0	168	39
V	5	1.66	–	1450	40[a]	40[a]	1.88[a]	1.70	41.6	135	47
B&V	5	1.54	347	1460	40[a]	40[a]	1.88[a]	1.65	40.0	195	32
No B&V	10	1.70	–	–	40[a]	40[a]	1.88[a]	1.91	48.8	124	62
B	10	1.60	347	–	33	40[a]	1.88[a]	1.57	40.0	168	38
V	10	1.65	–	1300	40[a]	40[a]	1.88[a]	1.71	41.5	134	47
B&V	10	1.54	347	1350	40[a]	40[a]	1.88[a]	1.60	40.0	197	31
No B&V	25	1.69	–	–	40[a]	40[a]	1.88[a]	1.91	48.8	124	62
B	25	1.59	347	–	34	40[a]	1.88[a]	1.62	40.0	171	37
V	25	1.65	–	1250	40[a]	40[a]	1.88[a]	1.74	41.9	134	47
B&V	25	1.54	347	1280	40[a]	40[a]	1.88[a]	1.65	40.0	197	31

[a] Bound.

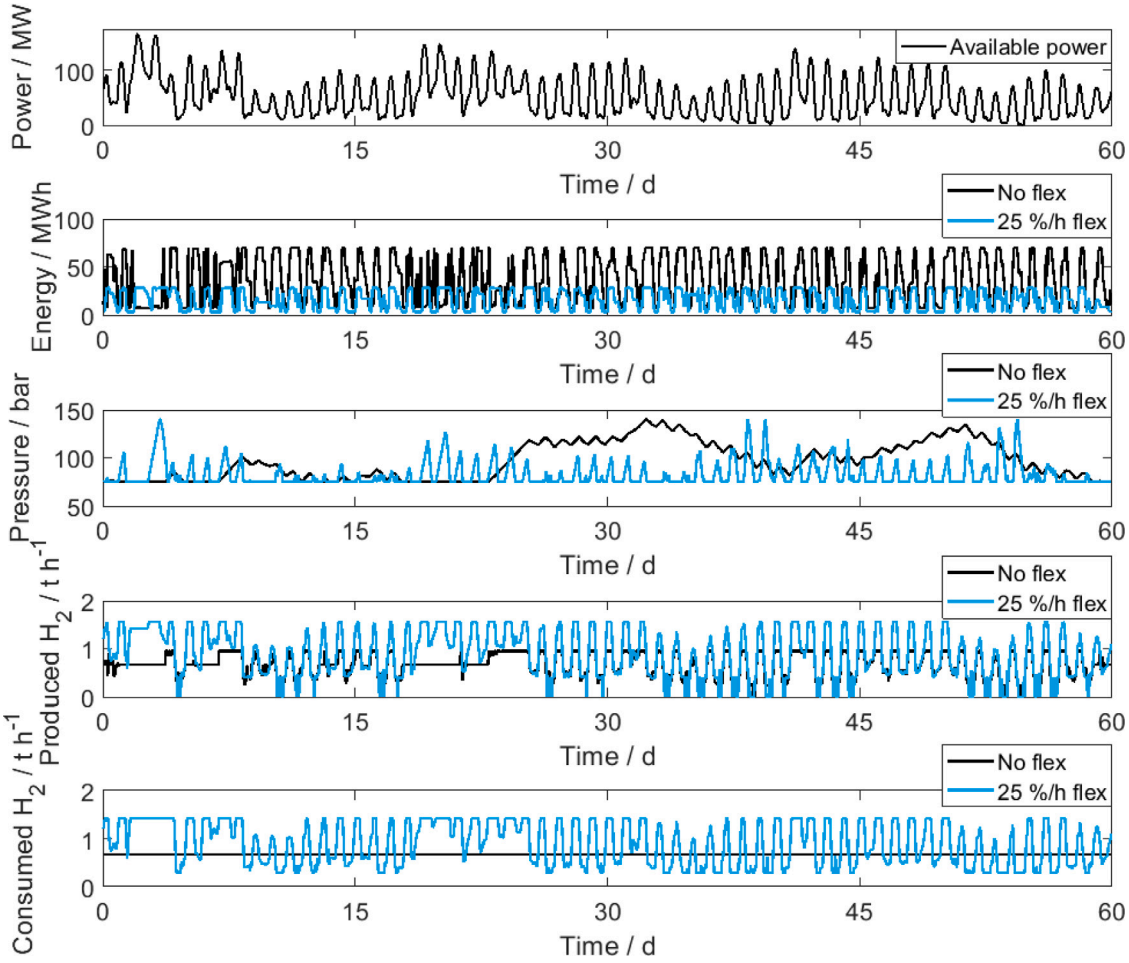

Fig. A.6. Energy content of the battery, H_2 pressure inside the H_2 vessel, H_2 produced by the electrolyzer, and H_2 converted in the methanol plant for the 'No flexibility' and '25%/h flexibility' cases for the current unit cost scenario. The power availability profile (May-Jun scenario) is also shown to better interpret the optimal scheduling.

different power generation scenarios, i.e., a winter generation profile dominated by wind production and a summer generation profile with high peaks due to PV generation, the optimal design of the Power-to-Methanol plants does not have extreme differences. This might be due to the similar size of the photovoltaic and wind power plants and to the complementarity effect of renewables, which affects the need for storage and the costs [26,28].

Figures A.6 and A.7 show how the battery and the H_2 storage are optimally operated for the considered scenarios. Both storage technologies are operated on a daily basis to cope with the high power peaks due to the PV generation during the May–Jun scenario (Fig. A.6) when flexibility of the methanol synthesis plant is allowed. In fact, the possibility of varying the methanol production rate in periods of renewable production shortage reduces the need for high amounts of stored hydrogen and long-term storage. A similar operation can be noticed for the Nov–Dec scenario (Fig. A.7). The main difference lies in the longer duration of the 'hold phase' of both storage technologies, and it is probably due to the scenario, which is characterized by a relevant wind power generation that has different characteristic times from PV generation. Nevertheless, these hold phases last a few days at most since the methanol synthesis plant is assumed to be always operating.

The duration of the 'hold phase' of storage suggests that shorter time frames could have been considered for scheduling. Nevertheless, even longer time frames would allow for taking into account the seasonality of power generation in the design phase. This aspect is particularly evident from the design differences when considering two power generation profiles of the same renewable park in two periods of the year (Table A.10). In fact, the optimal design of the Power-to-Methanol plant for the Nov–Dec scenario leads to a higher production cost of methanol when the plant is optimally operated in the May–Jun scenario (1.43 €/kg instead of 1.39 €/kg). Nevertheless, the relative difference between the methanol production cost for the two power generation scenarios is probably lower than the level of uncertainty of the model, thus meaning that considering a 2-month scenario for scheduling in the design phase already provides good indications of suitable plant designs. However, this might be not true when the ratio between the installed capacity of wind power and photovoltaic plants is quite different, and long-term hydrogen storage, e.g., a liquid organic hydrogen carrier [28], could be needed.

Finally, Table A.10 shows that an already moderate flexibility of the methanol plant increases the consumption of the generated renewable energy (P_{renew} in the table), thus reducing the renewable curtailment: a ramp rate of 5%/h already increases the renewable energy utilization from 66%–72% to 93%–94%. In the Nov–Dec scenario with current unit costs and a maximum ramp rate of the methanol plant of 25%/h, a slight decrease of the renewable curtailment (93% instead of 95%) can be noticed compared to the case with 5%/h as ramp rate. This result can be explained by the lower size of the electrolyzer and methanol synthesis units probably due to a locally optimal solution.

Table A.10
Optimization results for the stand-alone case study for the considered scenarios (May–Jun and Nov–Dec, and current and future unit cost).

	Flexibility %/h	Specific cost of MeOH €/kg	En_{batt} MWh	V m^3	N_{mod} –	p_{PEM} bar	β_{max} –	$\dot{m}_{H_{2,MeOH},nom}$ t/h	$MeOH_y$ kt	$CAPEX_0$ M€	$OPEX_y$ M€	P_{renew} %
May–Jun	0	1.78	70	5000	20	40[a]	3.5[a]	0.67	28.3	350	2	71%
May–Jun	5	1.40	27	800	33	40[a]	3.5[a]	1.43	37.9	350	3	93%
May–Jun	25	1.39	28	510	33	40[a]	3.5[a]	1.43	37.9	349	3	93%
Nov–Dec	0	2.38	35	5930	15	40[a]	3.5[a]	0.46	19.5	329	2	66%
Nov–Dec	5	1.70	23	940	28	40[a]	3.5[a]	1.22	29.2	335	2	95%
Nov–Dec	25	1.69	17	840	26	40[a]	3.5[a]	1.15	28.5	327	2	93%
Future unit cost scenario												
May–Jun	0	1.57	100	4500	20	40[a]	3.5[a]	0.68	28.8	312	2	72%
May–Jun	5	1.27	30	810	33	40[a]	3.5[a]	1.45	38.0	317	3	93%
May–Jun	25	1.26	37	500	33	40[a]	3.5[a]	1.45	38.1	316	3	93%
Nov–Dec	0	2.10	36	6300	16	40[a]	3.5[a]	0.48	20.0	298	2	69%
Nov–Dec	5	1.53	22	820	27	40[a]	3.5[a]	1.19	28.9	298	2	94%
Nov–Dec	25	1.53	16	880	27	40[a]	3.5[a]	1.18	28.8	298	2	94%

[a] Bound.

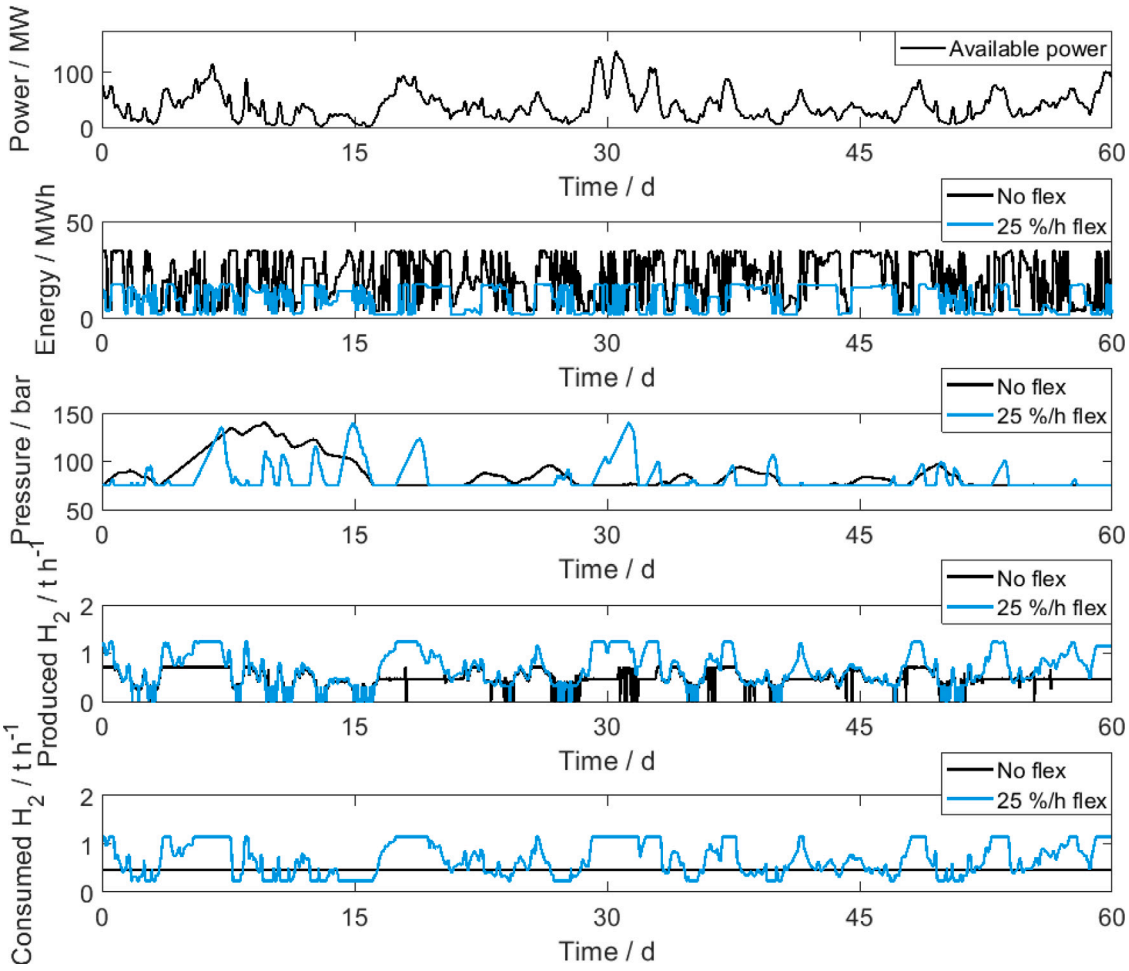

Fig. A.7. Energy content of the battery, H_2 pressure inside the H_2 vessel, H_2 produced by the electrolyzer, and H_2 converted in the methanol plant for the 'No flexibility' and '25%/h flexibility' cases for the current unit cost scenario. The power availability profile (Nov–Dec scenario) is also shown to better interpret the optimal scheduling.

Appendix B. Supplementary data

Supplementary material related to this article can be found online at https://doi.org/10.1016/j.est.2023.108614.

References

[1] Konstantin Räuchle, Ludolf Plass, Hans-Jürgen Wernicke, Martin Bertau, Methanol for renewable storage and utilization, Energy Technol. 4 (2016) 193–200, http://dx.doi.org/10.1002/ente.201500322.

[2] International Renewable Energy Agency (IRENA), Electricity Storage and Renewables: Costs and Markets to 2030, 2017.

[3] International Renewable Energy Agency (IRENA) and Methanol Institute, Innovation Outlook: Renewable Methanol, Abu Dhabi, 2021.

[4] Kirsten Ulonska, Andrea König, Marten Klatt, Alexander Mitsos, Jörn Viell, Optimization of multiproduct biorefinery processes under consideration of biomass supply chain management and market developments, Ind. Eng. Chem. Res. 57 (20) (2018) 6980–6991, http://dx.doi.org/10.1021/acs.iecr.8b00245.

[5] Malek Khadraoui, Ramzi Khiari, Latifa Bergaoui, Evelyne Mauret, Production of lignin-containing cellulose nanofibrils by the combination of different mechanical processes, Ind. Crops Prod. 183 (2022) 114991, http://dx.doi.org/10.1016/j.indcrop.2022.114991.

[6] Niklas Von Der Assen, Leonard J. Müller, Annette Steingrube, Philip Voll, André Bardow, Selecting CO_2 sources for CO_2 utilization by environmental-merit-order curves, Environ. Sci. Technol. 50 (3) (2016) 1093–1101, http://dx.doi.org/10.1021/acs.est.5b03474.

[7] International Energy Agency (IEA), Renewables 2022: Analysis and Forecast to 2027, Paris, 2022.

[8] Vincent Dieterich, Alexander Buttler, Andreas Hanel, Hartmut Spliethoff, Sebastian Fendt, Power-to-liquid via synthesis of methanol, DME or Fischer–Tropsch-fuels: a review, Energy Environ. Sci. 13 (2020) 3207–3252, http://dx.doi.org/10.1039/d0ee01187h.

[9] Xiaoti Cui, Søren Knudsen Kær, Mads Pagh Nielsen, Energy analysis and surrogate modeling for the green methanol production under dynamic operating conditions, Fuel 307 (2022) 121924, http://dx.doi.org/10.1016/j.fuel.2021.121924.

[10] Simone Mucci, Alexander Mitsos, Dominik Bongartz, Power-to-X processes based on PEM water electrolyzers: A review of process integration and flexible operation, Comput. Chem. Eng. 175 (2023) 108260, http://dx.doi.org/10.1016/j.compchemeng.2023.108260.

[11] Qi Zhang, Ignacio E. Grossmann, Enterprise-wide optimization for industrial demand side management: Fundamentals, advances, and perspectives, Chem. Eng. Res. Des. 116 (2016) 114–131, http://dx.doi.org/10.1016/j.cherd.2016.10.006.

[12] Pascal Schäfer, Torben M. Daun, Alexander Mitsos, Do investments in flexibility enhance sustainability? A simulative study considering the German electricity sector, AIChE J. 66 (2020) 1–14, http://dx.doi.org/10.1002/aic.17010.

[13] Jannik Burre, Dominik Bongartz, Luisa Brée, Kosan Roh, Alexander Mitsos, Power-to-X: Between electricity storage, e-production, and demand side management, Chem.-Ingenieur-Techn. 92 (1–2) (2020) 74–84, http://dx.doi.org/10.1002/cite.201900102.

[14] Kosan Roh, Luisa C. Brée, Karen Perrey, Andreas Bulan, Alexander Mitsos, Optimal oversizing and operation of the switchable chlor-alkali electrolyzer for demand side management, Comput. Aided Chem. Eng. 46 (2019) 1771–1776, http://dx.doi.org/10.1016/B978-0-12-818634-3.50296-4.

[15] Jachin Gorre, Felix Ortloff, Charlotte van Leeuwen, Production costs for synthetic methane in 2030 and 2050 of an optimized Power-to-Gas plant with intermediate hydrogen storage, Appl. Energy 253 (2019) 113594, http://dx.doi.org/10.1016/j.apenergy.2019.113594.

[16] Alexander Tremel, Electricity-based fuels, in: SpringerBriefs in Applied Sciences and Technology, Springer, Cham, 2018, http://dx.doi.org/10.1007/978-3-319-72459-1.

[17] Andrew Allman, Prodromos Daoutidis, Optimal scheduling for wind-powered ammonia generation: Effects of key design parameters, Chem. Eng. Res. Des. 131 (2018) 5–15, http://dx.doi.org/10.1016/j.cherd.2017.10.010.

[18] Ganzhou Wang, Alexander Mitsos, Wolfgang Marquardt, Renewable production of ammonia and nitric acid, AIChE J. 66 (2020) 1–9, http://dx.doi.org/10.1002/aic.16947.

[19] Luis Valverde, Carlos Bordons, Felipe Rosa, Integration of fuel cell technologies in renewable-energy-based microgrids optimizing operational costs and durability, IEEE Trans. Ind. Electron. 63 (1) (2016) 167–177, http://dx.doi.org/10.1109/TIE.2015.2465355.

[20] Paolo Gabrielli, Matteo Gazzani, Emanuele Martelli, Marco Mazzotti, Optimal design of multi-energy systems with seasonal storage, Appl. Energy 219 (2018) 408–424, http://dx.doi.org/10.1016/j.apenergy.2017.07.142.

[21] Jachin Gorre, Fabian Ruoss, Hannu Karjunen, Johannes Schaffert, Tero Tynjälä, Cost benefits of optimizing hydrogen storage and methanation capacities for Power-to-Gas plants in dynamic operation, Appl. Energy 257 (2020) 113967, http://dx.doi.org/10.1016/j.apenergy.2019.113967.

[22] Jiarong Li, Jin Lin, Yonghua Song, Capacity optimization of hydrogen buffer tanks in renewable power to ammonia (P2A) system, in: 2020 IEEE Power & Energy Society General Meeting, PESGM, IEEE, 2020, pp. 1–5.

[23] S. Schulte Beerbühl, M. Fröhling, F. Schultmann, Combined scheduling and capacity planning of electricity-based ammonia production to integrate renewable energies, European J. Oper. Res. 241 (3) (2015) 851–862, http://dx.doi.org/10.1016/j.ejor.2014.08.039.

[24] Ola Osman, Sgouris Sgouridis, Andrei Sleptchenko, Scaling the production of renewable ammonia: A techno-economic optimization applied in regions with high insolation, J. Clean. Prod. 271 (2020) 121627, http://dx.doi.org/10.1016/j.jclepro.2020.121627.

[25] Andrew Allman, Matthew J. Palys, Prodromos Daoutidis, Scheduling-informed optimal design of systems with time-varying operation: A wind-powered ammonia case study, AIChE J. 65 (7) (2019) http://dx.doi.org/10.1002/aic.16434.

[26] Chao Chen, Aidong Yang, René Bañares-Alcántara, Renewable methanol production: Understanding the interplay between storage sizing, renewable mix and dispatchable energy price, in: Advances in Applied Energy, Vol. 2, 2021, http://dx.doi.org/10.1016/j.adapen.2021.100021.

[27] Chao Chen, Aidong Yang, Power-to-Methanol: The role of process flexibility in the integration of variable renewable energy into chemical production, Energy Convers. Manage. 228 (2021) 113673, http://dx.doi.org/10.1016/j.enconman.2020.113673.

[28] Tibor Svitnič Tibor, Kai Sundmacher, Renewable methanol production: Optimization-based design, scheduling and waste-heat utilization with the flux-max approach, Appl. Energy 326 (2022) 120017, http://dx.doi.org/10.1016/j.apenergy.2022.120017.

[29] General Algebraic Modeling System (GAMS), https://www.gams.com/ (last visit: 2023-05-19).

[30] Alexander Mitsos, Norbert Asprion, Christodoulos A. Floudas, Michael Bortz, Michael Baldea, Dominique Bonvin, Adrian Caspari, Pascal Schäfer, Challenges in process optimization for new feedstocks and energy sources, Comput. Chem. Eng. 113 (2018) 209–221, http://dx.doi.org/10.1016/j.compchemeng.2018.03.013.

[31] Aida Khajavirad, Nikolaos V. Sahinidis, A hybrid LP/NLP paradigm for global optimization relaxations, Math. Program. Comput. 10 (2018) 383–421, http://dx.doi.org/10.1007/s12532-018-0138-5.

[32] International Energy Agency (IEA), World energy outlook 2021, 2021.

[33] International Energy Agency (IEA), The future of hydrogen: Seizing today's opportunities, Technical report, Paris, 2019.

[34] Marcelo Carmo, David L. Fritz, Jürgen Mergel, Detlef Stolten, A comprehensive review on PEM water electrolysis, Int. J. Hydrogen Energy 38 (12) (2013) 4901–4934, http://dx.doi.org/10.1016/j.ijhydene.2013.01.151.

[35] M. Kopp, D. Coleman, C. Stiller, K. Scheffer, J. Aichinger, B. Scheppat, Energiepark Mainz: Technical and economic analysis of the worldwide largest Power-to-Gas plant with PEM electrolysis, Int. J. Hydrogen Energy 42 (2017) 13311–13320, http://dx.doi.org/10.1016/j.ijhydene.2016.12.145.

[36] Mohammad-Reza Tahan, Recent advances in hydrogen compressors for use in large-scale renewable energy integration, Int. J. Hydrogen Energy 47 (83) (2022) 35275–35292, http://dx.doi.org/10.1016/j.ijhydene.2022.08.128.

[37] Ramin Moradi, Katrina M. Groth, Hydrogen storage and delivery: Review of the state of the art technologies and risk and reliability analysis, Int. J. Hydrogen Energy 44 (23) (2019) 12254–12269, http://dx.doi.org/10.1016/j.ijhydene.2019.03.041.

[38] Ahmed M. Elberry, Jagruti Thakur, Annukka Santasalo-Aarnio, Martti Larmi, Large-scale compressed hydrogen storage as part of renewable electricity storage systems, Int. J. Hydrogen Energy 46 (29) (2021) 15671–15690, http://dx.doi.org/10.1016/j.ijhydene.2021.02.080.

[39] Michael Hirscher, Handbook of Hydrogen Storage, Wiley-VCH Verlag GmbH & Co. KGaA, Weinheim, Germany, 2010, http://dx.doi.org/10.1002/9783527629800.

[40] B. Anicic, P. Trop, D. Goricanec, Comparison between two methods of methanol production from carbon dioxide, Energy 77 (2014) 279–289, http://dx.doi.org/10.1016/j.energy.2014.09.069.

[41] Alvaro Gonzalez-Castellanos, David Pozo, Aldo Bischi, Detailed Li-ion battery characterization model for economic operation, Int. J. Electr. Power Energy Syst. 116 (2020) 105561, http://dx.doi.org/10.1016/j.ijepes.2019.105561.

[42] Lauri Järvinen, Pietari Puranen, Antti Kosonen, Vesa Ruuskanen, Jero Ahola, Pertti Kauranen, Michael Hehemann, Automized parametrization of PEM and alkaline water electrolyzer polarisation curves, Int. J. Hydrogen Energy 47 (75) (2022) 31985–32003, http://dx.doi.org/10.1016/j.ijhydene.2022.07.085.

[43] Anita H. Reksten, Magnus S. Thomassen, Steffen Møller-Holst, Kyrre Sundseth, Projecting the future cost of PEM and alkaline water electrolysers; a CAPEX model including electrolyser plant size and technology development, Int. J. Hydrogen Energy 47 (2022) 38106–38113, http://dx.doi.org/10.1016/j.ijhydene.2022.08.306.

[44] Yang He, Haisheng Chen, Yujie Xu, Jianqiang Deng, Compression performance optimization considering variable charge pressure in an adiabatic compressed air energy storage system, Energy 165 (2018) 349–359, http://dx.doi.org/10.1016/j.energy.2018.09.168.

[45] Roman G. Frank, Christian Wacker, Niehuis Reinhard, Loss characterization of advanced VIGV configurations with adjustable blade geometry, J. Turbomach. 144 (3) (2022) 031012, http://dx.doi.org/10.1115/1.4052409.

[46] Lorenz T. Biegler, Ignacio E. Grossmann, Arthur W. Westerberg, Systematic methods of chemical process design, Prentice Hall PTR, ISBN: 9780134924229, 1997.

[47] Pascal Schäfer, Artur M. Schweidtmann, Philipp H.A. Lenz, Hannah M.C. Markgraf, Alexander Mitsos, Wavelet-based grid-adaptation for nonlinear scheduling subject to time-variable electricity prices, Comput. Chem. Eng. 132 (2020) http://dx.doi.org/10.1016/j.compchemeng.2019.106598.

[48] BSE engineering, Power-to-Methanol at small-scale: Flexmethanol 10 MW & 20 MW module, http://www.wfbe.de/BSE-Flyer-BASF-DB_web.pdf (last visit: 2023-05-19).

[49] ENTSO-E transparency platform. ENTSO-E: Day ahead prices and power generation data, https://transparency.entsoe.eu/ (last visit: 2023-07-23).
[50] International Renewable Energy Agency (IRENA), Renewable power generation costs in 2021, 2022.
[51] Stefano Sollai, Andrea Porcu, Vittorio Tola, Francesca Ferrara, Alberto Pettinau, Renewable methanol production from green hydrogen and captured CO_2: A techno-economic assessment, J. CO_2 Util. 68 (2023) http://dx.doi.org/10.1016/j.jcou.2022.102345.
[52] Friedrich Kunz, Alexander Zerrahn, Benefits of coordinating congestion management in electricity transmission networks: Theory and application to Germany, Util. Policy 37 (2015) 34–45, http://dx.doi.org/10.1016/j.jup.2015.09.009.
[53] Yi Zheng, Chunjun Huang, Shi You, Yi Zong, Economic evaluation of a power-to-hydrogen system providing frequency regulation reserves: a case study of denmark, Int. J. Hydrogen Energy (2023) http://dx.doi.org/10.1016/j.ijhydene.2023.03.253.
[54] Pascal Schäfer, Hermann Graf Westerholt, Artur M. Schweidtmann, Svetlina Ilieva, Alexander Mitsos, Model-based bidding strategies on the primary balancing market for energy-intense processes, Comput. Chem. Eng. 120 (2019) 4–14, http://dx.doi.org/10.1016/j.compchemeng.2018.09.026.
[55] Pascal Schäfer, Nils Hansmann, Svetlina Ilieva, Alexander Mitsos, Model-based bidding strategies for simultaneous optimal participation in different balancing markets, Comput. Aided Chem. Eng. 46 (2019) 1639–1644, http://dx.doi.org/10.1016/B978-0-12-818634-3.50274-5.
[56] Mariano Martín, Methodology for solar and wind energy chemical storage facilities design under uncertainty: Methanol production from CO_2 and hydrogen, Comput. Chem. Eng. 92 (2016) 43–54, http://dx.doi.org/10.1016/j.compchemeng.2016.05.001.
[57] U.S. Department of energy (DOE). Technical targets for hydrogen delivery, https://www.energy.gov/eere/fuelcells/doe-technical-targets-hydrogen-delivery (last visit: 2023-05-19).
[58] Éverton S. Van-Dal, Chakib Bouallou, Design and simulation of a methanol production plant from CO_2 hydrogenation, J. Clean. Prod. 57 (2013) 38–45, http://dx.doi.org/10.1016/j.jclepro.2013.06.008.
[59] Kurt M. Vanden Bussche, Gilbert F. Froment, A steady-state kinetic model for methanol synthesis and the water gas shift reaction on a commercial $Cu/ZnO/Al_2O_3$, J. Catal. (161) (1996) 1–10, http://dx.doi.org/10.1006/jcat.1996.0156.
[60] Álvaro A. Ramírez-Santos, Christophe Castel, Eric Favre, Utilization of blast furnace flue gas: Opportunities and challenges for polymeric membrane gas separation processes, J. Membr. Sci. 526 (2017) 191–204, http://dx.doi.org/10.1016/j.memsci.2016.12.033.
[61] Kenneth M. Guthrie, Data and techniques for preliminary capital cost estimating, Chem. Eng. 3 (1969) 114–142.
[62] Natural gas utilization via small scale methanol technologies, in: ADI Analytics LLC, Houston, Texas, 2015, http://www.sgicc.org/uploads/8/4/3/1/8431164/bftp_methanol_white_paper_vf.pdf, (last visit: 2023-07-19).
[63] International Renewable Energy Agency (IRENA), Future of Solar Photovoltaic: Deployment, investment, technology, grid integration and socio-economic aspects, 2019.
[64] International Renewable Energy Agency (IRENA), Future of Wind: Deployment, investment, technology, grid integration and socio-economic aspects, 2019.